IN THE UNITED STATES PATENT AND TRADEMARK OFFICE

Appellant:	Jan E. Schnitzer		
Application No.:	10/056,230	Group:	1642
Filed:	January 24, 2002	Examiner:	S.N. Ungar
Confirmation No.:	6912		

For: TARGETING ENDOTHELIUM FOR TISSUE-SPECIFIC DELIVERY OF AGENTS

CERTIFICATE OF MAILING

I hereby certify that this correspondence is being deposited with the United States Postal Service with sufficient postage as First Class Mail in an envelope addressed to Commissioner for Patents, P.O. Box 1450, Alexandria, VA 22313-1450

on 4-22-05 Jennifer Warner
Date Signature

Jennifer Warner
Typed or printed name of person signing certificate

REPLY BRIEF

Mail Stop Appeal Brief-Patents
Commissioner for Patents
P.O. Box 1450
Alexandria, VA 22313-1450

Sir:

This Reply Brief is submitted in response to the Examiner's Answer mailed from the U.S. Patent and Trademark Office on February 22, 2005, for the above-referenced patent application. The issues are addressed in the order in which they were raised in the Examiner's Answer.

Issues and Claims Appealed

The Examiner is correct in that the claims on appeal are Claims 3-5, 7-9 and 12-14. The Examiner has also correctly set forth appealed Claim 9.

Appellant's Attorney acknowledges with thanks that one of the rejections of Claims 3-5, 7-9 and 12-14 under 35 U.S.C. 112, first paragraph (Issue 1) has been withdrawn. The remaining issues (Issue 2 and 3) are discussed below.

Issue 2 Rejection of Claims 3-5, 7-9 and 12-14 under 35 U.S.C. 112, first paragraph

The Examiner has maintained the rejection of Claims 3-5, 7-9 and 12-14, under 35 U.S.C. 112, first paragraph, stating that the Specification "did not reasonably provide enablement for a method of delivering any agent of interest across a luminal surface of vascular endothelium from one side of an underlying cell to another side in a tissue specific manner by binding to a component of caveolae on the luminal surface of the vascular endothelium in a tissue" (Examiner's Answer, p. 4). In particular, the Examiner has stated that identification of Mab 833 as a rat lung specific binder to a rat long specific component of caveolae was a hoped for but unexpected event, because "this type of effective specificity had not been previously attained" (Examiner's Answer, p. 5).

Appellant respectfully disagrees with this assessment. It is clear that Appellant has demonstrated the first 'proof of principle' that it is possible to target and deliver agents into and/or across a luminal surface of vascular endothelium in a tissue-specific manner. No one has previously demonstrated such delivery. However, it has been established previously that caveolae differ from tissue to tissue, and that certain proteins may be expressed primarily or solely in caveolae of certain types of tissues. See, for example, Tang, Z. et al., (J. Biol. Chem. 271(4):2255-61 (1996)), who indicate *inter alia* that caveolin-3 is expressed predominantly in muscle, attached hereto as Exhibit A; Feron, O. et al., (J. Biol. Chem 272(27):17744-8 (1997)), who mention antibodies to different tissue-specific types of caveolin, and also describe dynamic targeting of m2 muscarinic acetylcholine receptor to caveolae in cardiac myocytes, attached hereto as Exhibit B; and Scherer, P.E. et al., (J. Biol Chem. 272(46):29337-46 (1997)) who describe cell-type and tissue-specific expression of caveolin-2, attached hereto as Exhibit C. One of ordinary skill in the art would thus be aware that caveolae components can be tissue-specific. In view of these considerations, Appellants reiterate that undue experimentation would not be required to make and utilize agents that bind and localize to a component of caveolae in a tissue-specific manner, for use in the methods of the invention. One of ordinary skill in the art, using no more than routine experimentation, would be able to apply the methods of the invention to other antibodies or agents of interest which bind to and localize to components of the caveolae, for tissue-specific targeting of agents.

It should also be noted that actual reduction to practice is not required to prove enablement (*In re Gould v. Quigg*, 822 F.2d 1074, 1078, 3 USPQ 2d 1302, 1304 (Fed. Cir. 1987)), and that case law has indicated that a specification need not contain an example if the invention is otherwise disclosed in such a manner that one skilled in the art will be able to practice it without an undue amount of experimentation. *In re Borkowski*, 422 F.2d 904, 908, 164 USPQ 642, 645 (CCPA 1970). No undue experimentation is required to make and use the invention as claimed. Appellants describe all the necessary characteristics of the agent, namely that the agent must bind to a component of caveolae of the luminal surface of the vascular endothelium. One of ordinary skill in the art would be able to practice the invention using a variety of agents, using no more than routine experimentation. Thus, Appellant asserts that the claims are in fact enabled and respectfully request removal of the rejection.

Issue 3: Rejection of Claims 3-5, 7-9, 12-14 under 35 U.S.C. 112, first paragraph

The Examiner also maintained the rejection of Claims 3-5, 7-9 and 12-14 under 35 U.S.C. 112, first paragraph, stating that "[t]he written description in this case only sets forth a method of delivering an agent of interest comprising Mab 833 across a luminal surface of vascular endothelium from one side of an underlying cell to another side by binding to a component of caveolae, a 90 kDa antigen, on the luminal surface of the vascular endothelium..." (Examiner's Answer, p. 6). The Examiner additionally states that the application could meet the written description requirement if it provided a description of sites at which tissue specific caveolae are found, for example.

Appellant notes that it is not the caveolae themselves that are tissue-specific, but that certain components of caveolae are tissue-specific. Caveolae are well-defined cellular structures that are easily isolatable using methods known to those of ordinary skill in the art. Furthermore, as described above, several proteins are known to be primarily or exclusively found in caveolae of certain tissues. The antigens themselves, as well as their characteristics, will vary depending on the caveole of the tissue in which they are found. One of ordinary skill in the art, given the description in the application and the state of the art, would understand that a variety of antigens are present in caveolae in a tissue-specific manner, and would be able to make and use agents that bind to them (e.g., antibodies) using routine experimentation, for use in the methods of the

invention. In view of these considerations, the subject matter of the claims is sufficiently described in the specification to enable one of ordinary skill in the art to understand what is encompassed by the claims, and to practice the claimed invention without undue experimentation. .

CONCLUSION

For the reasons presented above and in Appellant's Brief On Appeal, Appellant respectfully requests the Board of Patent Appeals and Interferences to reverse all of the rejections currently maintained by the Examiner in the above-identified application.

Respectfully submitted,

HAMILTON, BROOK, SMITH & REYNOLDS, P.C.

By Doreen M. Hogle Reg. No. 36,361 for
Elizabeth W. Mata
Registration No. 38,236
Telephone: (978) 341-0036
Facsimile: (978) 341-0136

Concord, MA 01742-9133
Date: April 22, 2005

THE JOURNAL OF BIOLOGICAL CHEMISTRY

Vol. 271, No. 4, Issue of January 26, pp. 2255–2261, 1996
Printed in U.S.A.

Molecular Cloning of Caveolin-3, a Novel Member of the Caveolin Gene Family Expressed Predominantly in Muscle*

(Received for publication, September 27, 1995, and in revised form, November 10, 1995)

ZhaoLan Tang‡, Philipp E. Scherer‡§, Takashi Okamoto¶‖, Kenneth Song‡, Caryn Chu, D. Stave Kohtz**, Ikuo Nishimoto‡‡, Harvey F. Lodish‡ §§, and Michael P. Lisanti‡ ¶¶**

*From the ‡Whitehead Institute for Biomedical Research, Cambridge, Massachusetts 02142-1479, the ¶Shriners Hospitals for Crippled Children, Massachusetts General Hospital, Department of Anesthesia, Harvard Medical School, Boston, Massachusetts 02114, the **Department of Pathology, Mount Sinai School of Medicine, New York, New York 10029, the ‡‡Department of Medicine, Cardiovascular Research Center, Massachusetts General Hospital-East, Charlestown, Massachusetts 02129, and the §§Department of Biology, Massachusetts Institute of Technology, Cambridge, Massachusetts 02139*

Caveolin, a 21–24-kDa integral membrane protein, is a principal component of caveolar membranes *in vivo*. Caveolin interacts directly with heterotrimeric G-proteins and can functionally regulate their activity. Recently, a second caveolin gene has been identified and termed caveolin-2. Here, we report the molecular cloning and expression of a third member of the caveolin gene family, caveolin-3. Caveolin-3 is most closely related to caveolin-1 based on protein sequence homology; caveolin-1 and caveolin-3 are ~65% identical and ~85% similar. A single stretch of eight amino acids (FEDVIAEP) is identical in caveolin-1, -2, and -3. This conserved region may represent a "caveolin signature sequence" that is characteristic of members of the caveolin gene family. Caveolin-3 mRNA is expressed predominantly in muscle tissue types (skeletal muscle, diaphragm, and heart) and is selectively induced during the differentiation of skeletal C2C12 myoblasts in culture. In many respects, caveolin-3 is similar to caveolin-1: (i) caveolin-3 migrates in velocity gradients as a high molecular mass complex; (ii) caveolin-3 colocalizes with caveolin-1 by immunofluorescence microscopy and cell fractionation studies; and (iii) a caveolin-3-derived polypeptide functionally suppresses the basal GTPase activity of purified heterotrimeric G-proteins. Identification of a muscle-specific member of the caveolin gene family may have implications for understanding the role of caveolin in different muscle cell types (smooth, cardiac, and skeletal) as previous morphological studies have demonstrated that caveolae are abundant in these cells. Our results also suggest that other as yet unknown caveolin family members are likely to exist and may be expressed in a regulated or tissue-specific fashion.

Caveolae are flask-shaped plasma membrane invaginations (1). They are most conspicuous in adipocytes, endothelial cells, muscle cells, and fibroblasts, but are thought to exist in most cell types (2). The exact cellular function of caveolae remains unknown, although they have been implicated in endothelial transcytosis (3), potocytosis (4), and signal transduction (reviewed in Refs. 5 and 6). Purification of caveolae-enriched membrane fractions reveals several distinct classes of lipid-modified signaling molecules, including heterotrimeric G-proteins (α- and $\beta\gamma$-subunits), Src-like kinases, and Ras-related GTPases (7–13). Based on these observations, we have proposed the "caveolae signaling hypothesis," which states that compartmentalization of certain cytoplasmic signaling molecules within caveolar membranes could allow rapid and efficient coupling of activated receptors to more than one effector system (5, 7).

A 22-kDa integral membrane protein termed caveolin is a principal component of caveolae *in vivo* (14). Caveolin may act as a scaffolding protein within caveolar membranes. Caveolin exists as a high molecular mass homo-oligomer (~14–16 monomeric units per oligomer) (15, 16), and these purified caveolin homo-oligomers have the capacity to self-associate into caveolae-like structures (15). In this regard, caveolin could serve as an oligomeric docking site for organizing and concentrating certain caveolin-interacting proteins (such as heterotrimeric G-proteins) within caveolae (17). Caveolin interacts directly with G-protein α-subunits. Residues 82–101 of caveolin are most critical for this interaction, and a caveolin-derived polypeptide encoding these residues functionally suppresses the basal GTPase activity of purified heterotrimeric G-proteins, acting as a GDP dissociation inhibitor (GDI)[1] (17). Also, caveolin rapidly undergoes tyrosine phosphorylation in response to insulin stimulation and thus could serve as a regulated docking site for SH2 domain-containing molecules (18).

Caveolin appears to be important for the formation of caveolar membranes as caveolin expression levels correlate very well with the morphological appearance of caveolae. For example, (i) caveolin is most abundant in cell types that contain numerous caveolae, *i.e.* adipocytes, endothelial cells, smooth muscle cells, and fibroblasts (19); (ii) caveolin and caveolae are both induced ~10–25-fold during the differentiation of 3T3-L1 fibroblasts to the adipocyte form (20, 21); and (iii) caveolin levels are dramat-

* This work was supported in part by a grant from the W. M. Keck Foundation to the Whitehead Fellows program (to M. P. L.), National Institutes of Health FIRST Award GM-50443 (to M. P. L.), National Institutes of Health Grants GM-49516 and DK-47618 (to H. F. L.), and a grant from Bristol-Myers-Squibb (to I. N.). The costs of publication of this article were defrayed in part by the payment of page charges. This article must therefore be hereby marked "*advertisement*" in accordance with 18 U.S.C. Section 1734 solely to indicate this fact.

The nucleotide sequence(s) reported in this paper has been submitted to the GenBank™/EMBL Data Bank with accession number(s) U31968.

§ Supported by a Swiss National Science Foundation fellowship.

‖ Recipient of fellowships from the Byotai-Taisha Foundation and the Mochida Memorial Foundation.

¶¶ To whom correspondence should be addressed: Whitehead Inst. for Biomedical Research, 9 Cambridge Center, Cambridge, MA 02142-1479. Tel.: 617-258-5225; Fax: 617-258-9872; E-mail: lisanti@wi.mit.edu.

[1] The abbreviations used are: GDI, GDP dissociation inhibitor; MDCK, Madin-Darby canine kidney; Mes, 4-morpholineethanesulfonic acid; MBS, Mes-buffered saline; PBS, phosphate-buffered saline; GAP, GTPase-activating protein; GTPγS, guanosine 5′-*O*-(3-thiotriphosphate).

ically reduced and caveolae are morphologically absent in cells transformed by various activated oncogenes, including v-*abl* and activated *ras* (22). However, there are certain cell lines that morphologically contain caveolae, but fail to express caveolin (7). This finding has suggested that other caveolin-related proteins may exist that are immunologically distinct from caveolin.

Two discrete isoforms of caveolin are known to exist: α-caveolin contains residues 1–178, while β-caveolin contains residues 32–178 (23). These isoforms are derived from a single gene through alternate initiation during translation. More specifically, methionine 32 serves as an internal translation initiation site to generate β-caveolin (23). Although these two isoforms are functionally identical in many respects, they assume a distinct but overlapping subcellular distribution within a single cell (23), and only β-caveolin is phosphorylated on serine residues *in vivo* (21). Thus, coexpression of α- and β-caveolins may serve to generate or mark distinct subpopulations of caveolae that are differentially regulated by an unknown caveolin-associated serine kinase (23).

A second mechanism exists for generating caveolin diversity. A novel caveolin-related protein has recently been identified. This protein, termed caveolin-2, is the product of a separate gene (24). Thus, caveolin (re-termed caveolin-1) is the first member of a multigene family. As both caveolin-1 and caveolin-2 have a relatively restricted tissue distribution (24), this suggested to us that other caveolin genes should exist.

Here, we report the molecular cloning, sequence, and tissue-specific expression of a third novel member of the caveolin gene family, caveolin-3. The current discovery of tissue-specific caveolin genes may end or at least alter the debate regarding the existence of caveolae without caveolin. Thus, a lack of caveolin expression (now known as caveolin-1) may simply reflect tissue-specific expression of different caveolin genes for which the appropriate probes have not yet been generated.

EXPERIMENTAL PROCEDURES

Materials—A monoclonal antibody (2297) directed against caveolin-1 was the generous gift of Dr. John R. Glenney (Transduction Laboratories, Lexington, KY). A rabbit polyclonal antibody directed against the C-terminal 44 amino acids of caveolin-1 (residues 135–178) was as characterized previously (23). This antibody specifically recognizes both α- and β-isoforms of caveolin-1, but does not recognize caveolin-2 or caveolin-3. The monclonal antibody 9E10 was provided by the Harvard Monoclonal Antibody Facility (Cambridge, MA). A variety of other reagents were purchased commercially: purified rat genomic DNA (Promega), a rat heart λgt11 cDNA library (CLONTECH), fetal bovine serum (JRH Biosciences), prestained protein markers (Life Technologies, Inc.), and Slow-Fade anti-fade reagent (Molecular Probes, Inc., Eugene, OR). Peptide synthesis was performed by the Biopolymers Facility at the Massachusetts Institute of Technology.

Northern Analysis of Tissues and cDNA Cloning—mRNA isolation from tissues as well as agarose gel electrophoresis and transfer to nylon membranes were performed as described (25). Hybridizations were performed in 50% formamide, 5 × SSC, 25 mM sodium phosphate, pH 7.0, 10 × Denhardt's solution, 5 mM EDTA, 1% SDS, 0.1 mg/ml poly(A) at 42 °C overnight and subsequently washed in 2 × SSC, 0.1% SDS and in 0.5 × SSC, 0.1% SDS at 50 °C. Radiolabeled DNA concentrations were at 2×10^6 cpm/ml. To obtain the rat caveolin-3 cDNA, a rat heart cDNA library (λgt11) was screened using a polymerase chain reaction-generated probe (see "Results") essentially as described previously for caveolin-1 (26). Automated DNA sequencing was performed by the Molecular Biology Core Facility at the Dana-Farber Cancer Institute.

Culture and Differentiation of C2C12 Skeletal Myoblasts—C2C12-3 cells (27) were derived from a single colony of C2C12 cells (28) cultured at clonal density and display a more stable phenotype than the parental cell line. C2C12-3 myoblasts were cultured as described elsewhere (27). Briefly, proliferating C2C12-3 cells were cultured in high mitogen medium (Dulbecco's modified Eagle's medium containing 15% fetal bovine serum and 1% chicken embryo extract) and induced to differentiate at confluence in low mitogen medium (Dulbecco's modified Eagle's medium containing 3% horse serum). Overt differentiation was indicated by the assembly of multinucleated syncytia, which commenced 36–48 h after the cells were switched to low mitogen medium. For Northern analysis, mRNA was isolated from proliferating C2C12-3 myoblasts in high mitogen medium at 50% confluence or from differentiated cells cultured at confluence in low mitogen medium for 48 h (27). Total cellular RNA was extracted with guanidine isothiocyanate and isolated by cesium chloride density centrifugation (29). mRNA was enriched by oligo(dT)-cellulose affinity chromatography and resolved by formaldehyde gel electrophoresis (30).

Recombinant Expression and Selection of Stable Cell Lines—An epitope-tagged form of caveolin-3 was subcloned into the MCS of the vector pCB7 (containing the hygro^R marker; gift of J. Casanova, Massachusetts General Hospital) for expression in COS-7 or MDCK cells. The *myc* epitope tag was incorporated into the C terminus (caveolin-3-GGEQKLISEEDLN) of the cloned rat caveolin-3 cDNA using polymerase chain reaction primers; GG was placed as a spacer between the epitope and the caveolin-3 coding sequences, as performed previously for caveolin-1 and caveolin-2 (23, 24, 31, 32). Constructs were transiently transfected into COS-7 cells by the DEAE-dextran method (33). In addition, MDCK cells were stably transfected using a modification of the calcium phosphate precipitation procedure, as we described previously (13, 23). After selection in medium supplemented with 400 μg/ml hygromycin B, resistant colonies were picked by trypsinization using cloning rings. Individual clones were screened by immunofluorescence and immunoblotting. Caveolin-3 expression in MDCK cells was detected using monoclonal antibody 9E10, which recognizes the *myc* epitope (EQKLISEEDLN).

Velocity Gradient Centrifugation—Estimation of the molecular mass of caveolin-3 was performed as described previously for caveolin-1 (15). Briefly, samples were dissociated by incubation with 500 μl of Mes-buffered saline (MBS; 25 mM Mes, pH 6.5, 0.15 M NaCl) plus 60 mM octyl glucoside. Solubilized material was then loaded atop a 5–40% linear sucrose gradient (4.3 ml) and centrifuged at 50,000 rpm (~340,000 × *g*) for 10 h in an SW 60 rotor (Beckman Instruments). Note that the entire gradient was prepared in MBS plus 60 mM octyl glucoside. After centrifugation, gradient fractions were collected from the top. Molecular mass standards for velocity gradient centrifugation were as follows: carbonic anhydrase (29 kDa), bovine serum albumin (66 kDa), alcohol dehydrogenase (150 kDa), β-amylase (200 kDa), and apoferritin (443 kDa) (Sigma).

Immunofluorescence—All reactions were performed at room temperature. COS-7 cells (cotransfected with cDNAs for caveolin-1 and caveolin-3) were briefly washed three times with PBS and fixed for 45 min in PBS containing 3% paraformaldehyde, 10 mM $NaIO_4$, and 70 mM lysine HCl. Fixed cells were rinsed with PBS and treated with 100 mM NH_4Cl in PBS for 10 min to quench free aldehyde groups. Cells were then permeabilized with 0.1% Triton X-100 for 10 min either at room temperature or on ice and washed with PBS (four times, 10 min each). The cells were then successively incubated with PBS, 2% bovine serum albumin containing the following: (i) 50 μg/ml each of normal goat IgG and donkey IgG, (ii) a 1:300 dilution of monoclonal antibody 9E10 and 40 μg/ml anti-caveolin-1 C terminus-specific polyclonal IgG, and (iii) lissamine rhodamine B sulfonyl chloride-conjugated goat anti-mouse antibody (5 μg/ml) and fluorescein isothiocyanate-conjugated donkey anti-rabbit antibody (5 μg/ml). The first incubation was for 30 min, while primary and secondary antibody reactions were for 60 min each. Cells were washed three time with PBS between incubations. Slides were mounted with Slow-Fade anti-fade reagent and observed under a Bio-Rad MR600 confocal fluorescence microscope.

Cell Fractionation—MDCK cells (recombinantly expressing caveolin-3) were grown to confluence in 150-mm dishes and used to prepare caveolin-enriched membrane fractions essentially as described (7, 8, 21, 34). Briefly, MDCK cells from a confluent 150-mm dish were scraped into 2 ml of MBS containing 1% Triton X-100 and 1 mM phenylmethylsulfonyl fluoride. Homogenization was carried out initially with 10 strokes of a loose-fitting Dounce homogenizer, followed by a Polytron tissue grinder (three 10-s bursts; Brinkmann Instruments). The homogenate was adjusted to 40% sucrose by addition of 2 ml of 80% sucrose prepared in MBS and placed at the bottom of an ultracentrifuge tube. A 5–30% linear sucrose gradient was formed above the homogenate and centrifuged at 39,000 rpm for 16–20 h in an SW 41 rotor (Beckman Instruments). A light-scattering band confined to the 15–20% sucrose region was harvested, diluted 3-fold with MBS, and pelleted in a microcentrifuge (14,000 × *g*, 15 min, 4 °C). The majority of protein remained within the 40% sucrose region of the gradient. Approximately 4–6 μg of caveolin-enriched domains were obtained from one 150-mm dish of MDCK cells representing 10 mg of protein, a yield of ~0.05% relative to the homogenate. We (7, 8, 13, 21) and others (34, 35) have

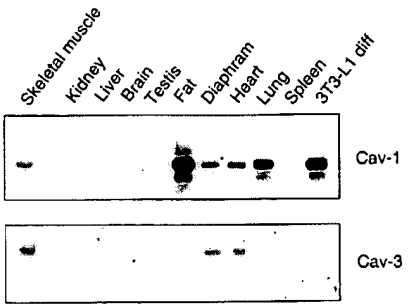

FIG. 1. **Northern blot analysis of the tissue distribution of caveolin-3.** Each lane contains 1 μg of poly(A)$^+$ RNA prepared from a given tissue. Blots were probed with the caveolin-1 cDNA, stripped, and reprobed with caveolin-3. Caveolin-1 and caveolin-3 mRNAs have different transcript sizes: ~2.5 kilobases for caveolin-1 and ~1.2 kilobases for caveolin-3. After the initial hybridizations, the blot was stripped and reprobed with a cytosolic hsp70 cDNA as a control for equal loading (as we published previously (21)).

demonstrated that these domains exclude a variety of organelle-specific membrane markers (for the endoplasmic reticulum, Golgi apparatus, lysosomes, mitochondria, and non-caveolar plasma membrane), but are dramatically enriched ~2000-fold in caveolin-1, a caveolar marker protein.

Immunoblotting of Gradient Fractions—Gradient fractions were separated by SDS-polyacrylamide gel electrophoresis (10% acrylamide) and transferred to nitrocellulose. After transfer, nitrocellulose sheets were stained with Ponceau S to visualize protein bands and subjected to immunoblotting with anti-caveolin-1 IgG (monoclonal antibody 2297; 1:400) or with 9E10 ascites (1:500) to visualize *myc*-tagged caveolin-3. For immunoblotting, incubation conditions were as described by the manufacturer (Promega and Amersham Corp.), except we supplemented our blocking solution with both 1% bovine serum albumin and 1% non-fat dry milk (Carnation). The amount of caveolin-1 and caveolin-3 that remains associated with caveolin-enriched fractions was estimated by immunoblotting as described (8). Quantitation was performed with a Molecular Dynamics computing densitometer. To ensure that these estimates were made in the linear range, we used multiple autoradiographic exposures and monitored their linearity using the densitometer essentially as described (36).

GTP Hydrolysis Assays—Trimeric G_{i2} purified from bovine spleen was provided by T. Asano (37). Trimeric G_o purified from bovine brain was provided by T. Haga (38). Steady-state GTP hydrolysis activity was examined as we described previously (39). Briefly, the assay was performed for 20 min at 37 °C in the presence of 20 μM Mg^{2+} with 10 nM G-protein. The caveolin-3-derived polypeptide contained the sequence DGVWRVSYTTFTVSKYWCYR, corresponding to amino acids 55–74 of caveolin-3.

RESULTS

Identification and Molecular Cloning of the cDNA for Caveolin-3—To identify other putative members of the caveolin gene family, the protein sequence of caveolin-1 was used to search existing data bases. Through this approach, a rat genomic sequence (~350 nucleotides in length; GenBank™ accession number U15280) was identified that could potentially encode part of a novel caveolin-related protein. This short genomic sequence was present 3′ to the last exon of the rat oxytocin receptor gene and in the opposite orientation to the coding sequence for the oxytocin receptor. Oligonucletide primers (5′-CCGGCC**GAATTC**ATGATGTGATTGCGGACCGCGAG-3′ and 5′-CCGGCC**GGATCC**ATCACCTTAATGTTGCTCCAG-AC-3′; *Eco*RI and *Bam*HI restriction sites are in boldface, and target sequences are underlined) were designed and used to amplify this nucleotide sequence from purified rat genomic DNA by polymerase chain reaction. A fragment of the expected size was subcloned into the MCS of pBluescript II KS$^+$, and its identity was verified by DNA sequencing.

Fig. 1 shows the tissue distribution of an ~1.2-kilobase mRNA species that specifically hybridizes at high stringency with this novel genomic sequence. This mRNA is present only in skeletal muscle, diaphragm, and heart, suggesting muscle-specific expression of this novel gene product. The distribution of caveolin-1 mRNA is shown for comparison. In contrast, caveolin-1 mRNA is ~2.5 kilobases and is most highly expressed (in descending order) in white adipose tissue, lung, and muscle tissues. Thus, this presumptive caveolin-related protein appeared distinct from caveolin-1 in its mRNA size and tissue distribution. Also, it is important to note that detection of caveolin-1 mRNA within skeletal muscle tissue reflects its expression within the endothelial cells of the muscle tissue, but not in the muscle cells themselves (see "Discussion" for a more detailed explanation).

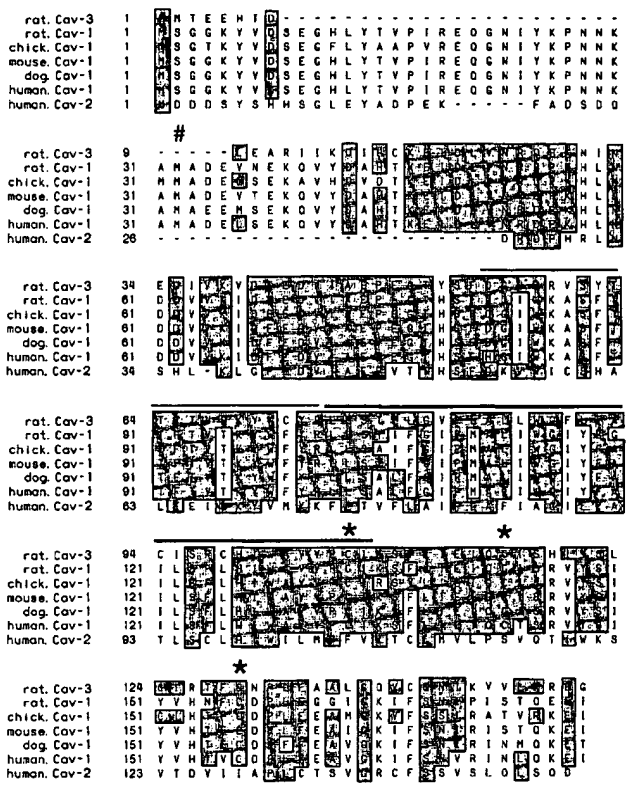

FIG. 2. **Deduced protein sequence of rat caveolin-3.** The protein sequence of rat caveolin-3 is compared with the known sequences of rat, chick, mouse, dog, and human caveolin-1 and with human caveolin-2. Residues identical to caveolin-3 are *boxed*. The position of the G-protein-binding region of caveolin-1 is *overlined*; the position of the hydrophobic membrane-spanning region is indicated by a *boldface overline*. A conserved methionine residue (an alternate start site in caveolin-1) and three conserved cysteine residues (sites of palmitoylation in caveolin-1) are indicated by the *pound sign* and *asterisks*, respectively.

To obtain the full-length cDNA, this polymerase chain reaction-generated genomic probe was used to screen a rat heart cDNA library (λgt11). Five independent positive clones were obtained from screening ~6×10^5 recombinant phage. Fig. 2 shows the predicted translation product of one of these positive cDNA clones. This full-length clone contained the same DNA sequence that was present within the probe used for screening. The open reading frame encodes a protein of 151 amino acids with a predicted molecular mass of 17,403.9 Da. It is smaller than rat caveolin-1, which is 178 amino acids and has a predicted molecular mass of 20,408.2 Da. We termed this protein caveolin-3. Data base searches with the deduced protein sequence of caveolin-3 revealed significant identity only to caveolin-1 and caveolin-2, but not to any other known proteins.

An alignment of sequences of rat caveolin-3 with caveolin-1 and caveolin-2 shows that caveolin-3 is more similar to caveo-

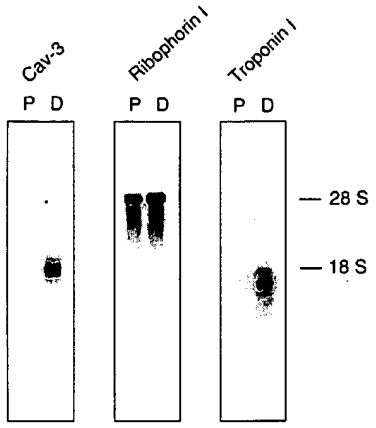

FIG. 3. **Induction of caveolin-3 mRNA during the differentiation of C2C12 skeletal myoblasts.** Each lane contains ~4 μg of poly(A)$^+$ RNA prepared from proliferating (*P*) or differentiated (*D*) C2C12 skeletal myoblasts. After initial hybridization with the cDNA for caveolin-3, the blot was stripped and reprobed with the ribophorin I cDNA as a control for equal loading and the troponin I (fast isoform) cDNA as a positive control for skeletal myoblast differentiation.

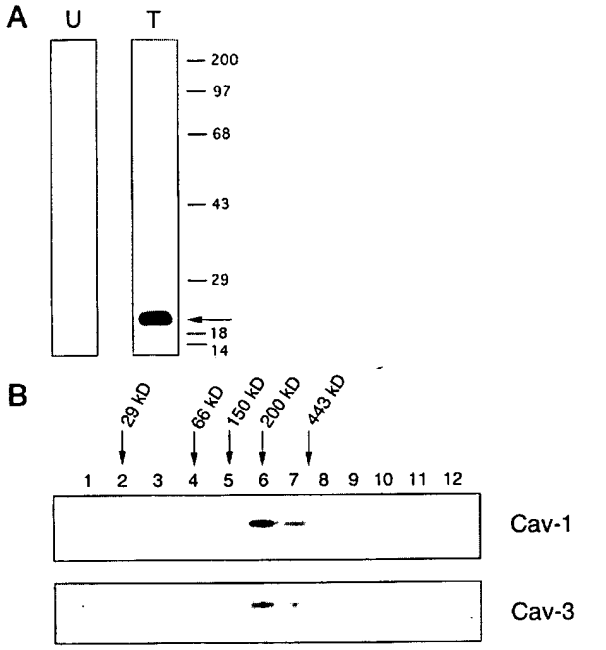

FIG. 4. **Recombinant expression of caveolin-3.** *A*, expression of *myc*-tagged caveolin-3 in COS-7 cells yielded a protein product of the expected molecular mass (~18–20 kDa). *U*, mock-transfected control; *T*, transfectants expressing caveolin-3. *B*, velocity gradient analysis of caveolin-3. Cells expressing *myc*-tagged caveolin-3 were solubilized, loaded atop a 5–40% sucrose gradient, and subjected to centrifugation for 10 h as we described previously for caveolin-1 (15). Note that caveolin-3 migrates mainly in fractions 6 and 7, identical to the migration of caveolin-1 shown for comparison. *Arrows* mark the positions of molecular mass standards. In *A* and *B*, expression of caveolin-3 was detected by immunblot analysis with monoclonal antibody 9E10, which recognizes the *myc* epitope (EQKLISEEDLN); caveolin-1 was detected using monoclonal antibody 2297.

lin-1 than to caveolin-2 (Fig. 2). Specifically, caveolin-1 and caveolin-3 are ~65% identical and ~85% similar based on conservative amino acid substitutions. A single stretch of eight amino acids (FEDVIAEP) is identical in caveolin-1, -2, and -3. This conserved region may represent a "caveolin signature sequence" that is characteristic of members of the caveolin gene family. In addition, the three cysteine residues that undergo palmitoylation in caveolin-1 (Fig. 2, see *asterisks*) (32) are absolutely conserved in caveolin-3, but not in caveolin-2. This suggests that caveolin-3 may be palmitoylated at these residues as well. Like caveolin-1, caveolin-3 contains a 33-amino acid membrane-spanning segment and a 44-amino acid C-terminal domain. However, the N-terminal domain of caveolin-3 is shorter than that of caveolin-1 by 27 amino acids. This fits well with the observation that two isoforms of caveolin-1 are generated by alternate translation initiation sites (methionines 1 and 32), yielding two protein products that differ in their extreme N terminus: caveolin-1α encoding residues 1–178 and caveolin-1β encoding residues 32–178 (23). Thus, caveolin-1β (147 amino acids) is approximately the same length as caveolin-2 (149 amino acids) and caveolin-3 (151 amino acids).

Caveolin-3 Is Induced during Differentiation of Skeletal Myoblasts in Culture—As caveolin-3 mRNA is most highly expressed in muscle tissue types (Fig. 1), we used C2C12 cells to examine if caveolin-3 expression is regulated during skeletal muscle differentiation. Cultured C2C12 cells offer a convenient system to study skeletal myoblast differentiation. These cells can be induced to differentiate from myoblasts into myotubes bearing an embryonic phenotype in low mitogen medium over a period of 2 days. As a positive control for differentiation, the expression of troponin I mRNA (fast isoform) was also monitored. The fast isoform of troponin I is expressed only in skeletal muscle cells, but not in cardiac muscle or other tissues (40). The constitutive expression of ribophorin I mRNA was monitored as a control for equal loading.

Compared with the constitutive expression of ribophorin I mRNA, caveolin-3 mRNA was undetectable in precursor myoblasts and strongly induced during myoblast differentiation (Fig. 3). Troponin I mRNA was dramatically induced to a similar extent as caveolin-3. These results are consistent with the selective expression of caveolin-3 mRNA in skeletal muscle and other muscle tissues (Fig. 1) and suggest that caveolin-3 may function in muscle from the earliest stages of its development.

Recombinant Expression of Caveolin-3—To study the properties of caveolin-3, we recombinantly expressed a *myc* epitope-tagged form of the protein. Caveolin-1 tagged with the *myc* epitope is functionally indistinguishable from endogenous caveolin-1 (23, 31, 32). Fig. 4*A* illustrates recombinant expression of *myc*-tagged caveolin-3. Expression of caveolin-3 yielded a protein product of the expected molecular mass (~18–20 kDa) that was slightly smaller than caveolin-1.

Caveolin-1 exists as an ~350-kDa homo-oligomer containing ~14–16 monomers per oligomer as shown using several approaches including velocity gradient centrifugation (15, 16). Oligomerization activity is localized to residues 61–101 of the cytoplasmic N-terminal domain of caveolin-1 (15); this 41-amino acid sequence is sufficient to confer oligomerization of the same stoichiometry upon a fusion protein (15). As only seven amino acid changes occur in this 41-amino acid stretch between caveolin-1 and caveolin-3 and six out of seven of these changes are conservative substitutions, caveolin-3 might also form well-defined high molecular mass homo-oligomers. To test this hypothesis, we used an established velocity gradient system developed previously to study oligomers of caveolin-1 (15). Like caveolin-1, caveolin-3 migrated as a high molecular mass complex between the 200- and 443-kDa molecular mass standards (Fig. 4*B*). In contrast, several other integral membrane proteins migrate at their expected monomeric molecular mass in these same velocity gradients (15).

The immunostaining pattern obtained with caveolin-3 is shown in Fig. 5 and is very similar to immunostaining patterns observed previously for caveolin-1 and caveolin-2 (7, 9, 14, 23, 24, 31). Many small micropatches are present throughout the

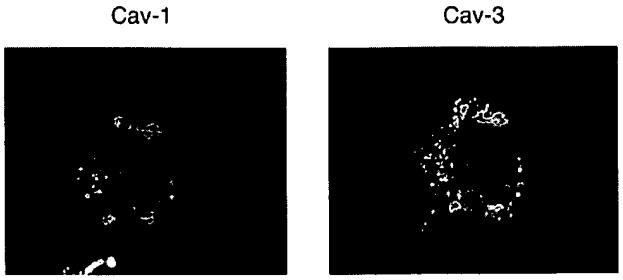

FIG. 5. **Immunolocalization of caveolin-1 and caveolin-3 within a single cell.** COS-7 cells were cotransfected with untagged caveolin-1 and *myc*-tagged caveolin-3. Cells expressing both caveolin gene products were selected for imaging by confocal laser fluorescence microscopy. Caveolin-1 expression was detected with a rabbit polyclonal IgG probe that specifically reacts only with caveolin-1; caveolin-3 expression was detected with monoclonal antibody 9E10, which recognizes the *myc* epitope. Control experiments employing singly transfected populations of COS-7 cells confirmed the specificity of these antibodies; no cross-reaction was observed (data not shown). Bound primary antibodies were visualized by incubation with distinctly tagged fluorescent secondary antibodies (fluorescein-conjugated for caveolin-1 and rhodamine-conjugated for caveolin-3; see "Experimental Procedures").

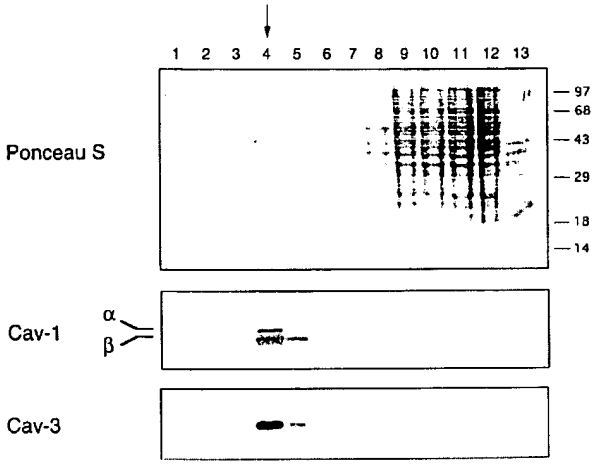

FIG. 6. **Subcellular fractionation of MDCK cells recombinantly expressing caveolin-3.** The distribution of total cellular proteins, caveolin-1, and caveolin-3 is shown. One-ml sucrose gradient fractions were collected from the top and analyzed by Ponceau S staining (*upper panel*) or immunoblotting (*lower panels*). Fractions 1–8 are the 5–30% sucrose layer, fractions 9–12 are the 40% sucrose layer, and fraction 13 is the insoluble pellet. Fractions 9–12 represent the "loading zone" of these bottom-loaded flotation gradients and contain the bulk of cellular membranes and cytosolic proteins (see "Experimental Procedures"). Note that fractions 4 and 5 retain >95% of caveolin-1 and caveolin-3 and exclude ~99.95% of total cellular proteins (based on independent protein determinations) and markers for the endoplasmic reticulum, Golgi apparatus, non-caveolar plasma membrane, mitochondria, and lysosomes as shown previously (7, 8, 21).

cell and along the cell surface. In addition, double-labeling experiments employing cells cotransfected with caveolin-1 and caveolin-3 demonstrate significant colocalization of these two distinct gene products (Fig. 5).

To further examine the colocalization of caveolin-1 and caveolin-3, we stably expressed caveolin-3 in MDCK cells, which contain endogenous caveolin-1. To separate membranes enriched in caveolin-1 from the bulk of cellular membranes and cytosolic proteins, an established equilibrium sucrose density gradient system was utilized (7, 8, 12, 13, 17, 18, 21, 23, 34, 35, 41). In this fractionation scheme, immunoblotting with anti-caveolin-1 IgG can be used to track the position of caveola-derived membranes within these bottom-loaded sucrose gradients. Using this procedure, caveolin-1 is purified ~2000-fold relative to total cell lysates as ~4–6 μg of caveolin-rich domains (containing ~90–95% of total cellular caveolin-1) are obtained from 10 mg of total MDCK proteins (13, 17). We (7, 8) and others (21) have shown that these caveolin-rich fractions exclude >99.95% of total cellular proteins and also markers for the non-caveolar plasma membrane, Golgi apparatus, lysosomes, mitochondria, and endoplasmic reticulum. Fig. 6 illustrates that in this fractionation scheme, ~90–95% of both caveolin-1 and caveolin-3 cofractionate and are targeted to the same low density fractions, suggesting that they colocalize to similar areas of the plasma membrane. This is consistent with results demonstrating their colocalization by fluorescence microscopy in intact cells (Fig. 5).

A Caveolin-3-derived Polypeptide Functionally Affects the GTPase Activity of Purified Heterotrimeric G-proteins—Caveolin-1 functionally interacts directly with G-protein α-subunits (17). Residues 82–101 of caveolin-1 are most critical for this interaction, and a caveolin-1-derived polypeptide encoding these residues can functionally suppress the basal GTPase activity of purified heterotrimeric G-proteins, apparently by inhibiting GDP/GTP exchange (17). Thus, this caveolin-1-derived peptide acts as a GDI for heterotrimeric G-proteins (17). This activity requires the complete caveolin-1 sequence from residues 82 to 101 as other peptides containing caveolin-1 residues 84–92 or 93–101 do not contain GDI activity[2]; also, a polypeptide derived from a caveolin-1 region that is not required for G-protein binding (residues 53–81) has no effect (17).

A region that corresponds to caveolin-1 residues 82–101 is present within caveolin-3 and is highly conserved (six amino acid changes occur in a 20-amino acid stretch; all six changes are conservative substitutions) (Fig. 2). Thus, the effect of the corresponding caveolin-3-derived polypeptide on the functional properties of purified trimeric G-proteins (G_o and G_{12}) was next evaluated. Fig. 7 shows the effect of the caveolin-3-derived polypeptide on the turnover number of GTPase activity of purified trimeric G-proteins. Like polypeptides derived from caveolin-1, this caveolin-3-derived polypeptide dose-dependently suppressed the GTPase activity of both trimeric G_o and G_{12} with IC_{50} values of 3 and 5 μM, respectively. A 10 μM concentration of this peptide yielded 80% inhibition for G_o and total inhibition for G_{12}. This is the same potency reported previously for the caveolin-1-derived polypeptide (17). However, unlike the caveolin-1-derived polypeptide, lower concentrations of the caveolin-3-derived polypeptide stimulated the GTPase activity. The steady-state GTPase activities of G_o and G_{12} were dose-dependently stimulated by nanomolar concentrations with EC_{50} values of 500 and 300 nM, respectively. Maximal stimulation was 1.6- and 1.3-fold over the basal activities of G_o and G_{12}, respectively. These findings are consistent with the recent observation that a polypeptide derived from the corresponding region of caveolin-2 selectively stimulates the GTPase activity of purified trimeric G-proteins, acting as a GTPase-activating protein (GAP) (24). Thus, this caveolin-3-derived polypeptide has both activities that are found separately in caveolin-1 and caveolin-2.

DISCUSSION

Caveolin-3 joins caveolin-1 and caveolin-2 as the third member of a growing caveolin gene family. As two forms of caveolin-1 (α- and β-isoforms) exist (23), there are now four distinct caveolin protein products (Fig. 8).

Caveolin-1, -2, and -3 all have a similar overall structure

[2] M. P. Lisanti and T. Okamoto, unpublished observations.

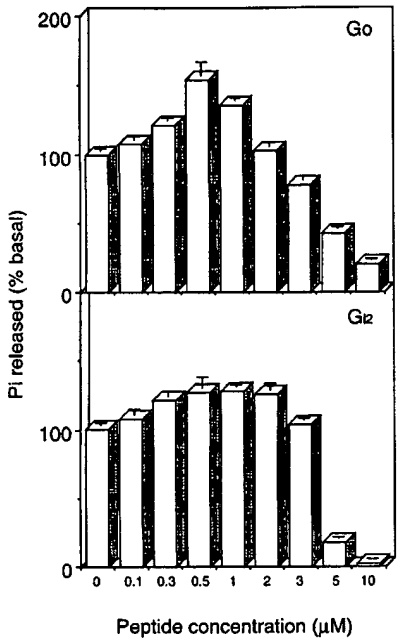

FIG. 7. **Effect of caveolin-3-derived polypeptides on the basal GTPase activity of purified heterotrimeric G-proteins.** *Upper*, trimeric G_o; *lower*, trimeric G_{i2}. The activity is expressed as a percentage of the basal activity, which was 0.17 ± 0.01 min^{-1} for G_o and 0.05 ± 0.005 min^{-1} for G_{i2} (mean ± S.E.; $n = 3$). All experiments were done independently three times, and the values indicate the means ± S.E.

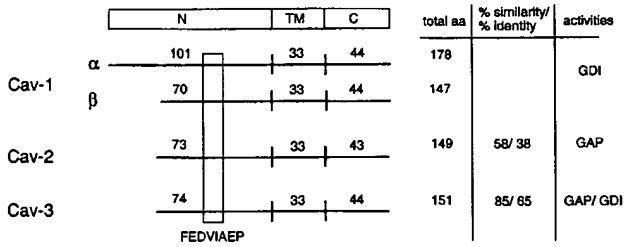

FIG. 8. **Schematic diagram summarizing known caveolin family members.** The overall structures of caveolin-1 (α- and β-isoforms), caveolin-2, and caveolin-3 are shown. All four protein products contain the invariant sequence FEDVIAEP within their hydrophilic N-terminal domains. Note that caveolin-1β (147 amino acids) is approximately the same length as caveolin-2 (149 amino acids) and caveolin-3 (151 amino acids); percent similarity and identity of caveolin-2 and caveolin-3 to caveolin-1 are shown. GDI and GAP activities are also noted. *TM*, transmembrane domain.

with a hydrophilic N-terminal domain, a 33-amino acid membrane-spanning segment, and a 43–44-amino acid hydrophilic C-terminal domain, and all three contain the invariant sequence FEDVIAEP within their N-terminal domains. These similarities predict that caveolin-2 and caveolin-3 should assume the same hairpin topology as caveolin-1; the N- and C-terminal domains of caveolin-1 are known to face the cytoplasm (23, 32, 42). Caveolin-2 and caveolin-3 colocalize with caveolin-1 when recombinantly expressed within a single cell (caveolin-1 and caveolin-2 (24); caveolin-1 and caveolin-3 (this report)), indicating that all three caveolins localize to caveolae. Based on sequence homology, caveolin-3 is most closely related to caveolin-1 and is most distant from caveolin-2. In accordance with this homology, both caveolin-1 (15, 16) and caveolin-3 (this report) form high molecular mass oligomers, while only a dimeric form of caveolin-2 has been detected (24).

Caveolin-1 and caveolin-2 are most highly expressed in white adipose tissue, and both are induced during adipocyte differentiation (21, 24); caveolin-3 is most highly expressed in muscle tissues and is induced during the differentiation of skeletal myoblasts in culture. This suggests that caveolin-1 and caveolin-2 may be very important for adipocyte function, while caveolin-3 is important for muscle cell types. The tissue-specific expression of different caveolin genes could help generate the formation of caveolae that are tailored to the function of a given cell type. For example, smooth muscle cell caveolae remain attached to the plasma membrane and are viewed as static structures, while endothelial cell caveolae detach from the plasma membrane and participate in endocytic and transcytotic transport events (1). The reason for these cell type-specific differences in the behavior of caveolae remains unknown; these differences could reflect tissue-specific expression of functionally distinct caveolin genes.

Prior to the identification of caveolin-3, we looked for expression of caveolin-1 in skeletal muscle fibers by immunofluorescence microscopy using four different caveolin-1-specific antibodies. Caveolin-1 expression was detected in surrounding endothelial cells, but not in skeletal muscle fibers,[3] explaining the apparent detection of small amounts of caveolin-1 mRNA in skeletal muscle tissue (Fig. 1, *upper panel*). Also, we were unable to detect caveolin-1 protein in differentiated or undifferentiated C2C12 skeletal myoblasts. As muscle cells contain caveolae, it appeared that caveolin-1 was not required for the formation of skeletal muscle cell caveolae. We also considered the possibility that a muscle-specific form of caveolin might exist that was not recognized by available caveolin-1 antibodies. However, we had no direct evidence to support this prediction. Our current observations that caveolin is a multigene family and that caveolin-3 mRNA is predominantly expressed in muscle tissues and differentiated C2C12 myoblasts may explain our inability to detect caveolin-1 in skeletal muscle fibers and C2C12 cells. Thus, a failure to detect caveolin-1 expression should not be interpreted as an absence of caveolae. For example, based on a lack of caveolin-1 expression, other investigators have concluded that caveolae do not exist in lymphocytes and neurons (43, 44). However, this predates the observation that caveolin is actually a multigene family of immunologically distinct but homologous molecules. Thus, other as yet undiscovered caveolin genes may exist that are expressed in lymphocytes and neuronal cells.

What could be the functional significance of caveolin diversity? Cell fractionation studies indicate that caveolin-1 copurifies with signal transducers, including G-proteins (7–12, 17, 23). Using an *in vitro* binding assay, caveolin-1 interacts directly with inactive G-protein α-subunits; this G-protein binding activity is located within residues 82–101 of the cytoplasmic N-terminal domain of caveolin-1 (17). A polypeptide containing caveolin-1 residues 82–101 functionally suppresses the basal activity of purified trimeric G-proteins by inhibiting GDP/GTP exchange, acting as a GDI for trimeric G-proteins (17). Conversely, the corresponding polypeptide from caveolin-2 acts as a GAP (24). As both caveolin-1 and caveolin-2 are coexpressed within the same cells, we have proposed that they could act in concert to recruit and sequester G-proteins in the GDP-liganded conformation within caveolae for presentation to activated G-protein-coupled receptors (24). More specifically, we have postulated that caveolin-2 would act first as a GAP to actively place the G-protein in the inactive GDP-bound state, and caveolin-1 would then act as a GDI to hold the G-protein in the inactive conformation by preventing GDP/GTP exchange (24). Here, we find that the corresponding caveolin-3-derived polypeptide has both activities found separately in caveolin-1

[3] M. P. Lisanti *et al.*, unpublished observations.

and caveolin-2; at nanomolar concentrations, the caveolin-3-derived polypeptide acts to stimulate the GTPase activity of purified trimeric G-proteins, and at micromolar concentrations, it suppresses their GTPase activity. Thus, caveolin-3 might subsume the functional roles of both caveolin-1 and caveolin-2 in certain muscle cell types.

We have previously evaluated the effect of over 200 polypeptides on the functional activities of purified trimeric G-proteins (39, 45–50), and the caveolin-derived peptides (Refs. 17 and 24 and this report) are the only polypeptides that produce GDI and/or GAP activities. However, many receptor-derived polypeptides contain GDP dissociation stimulator activity as expected, stimulating both GTPase activity and GTPγS binding at micromolar concentrations (39, 45–50).

It has been known for many years that caveolae are morphologically abundant in all muscle cell types (smooth, cardiac, and skeletal) (51–58). This appears to be relevant to the pathogenesis of Duchenne's muscular dystrophy. More specifically, (i) dystrophin has been localized to plasma membrane caveolae in smooth muscle cells (59), and (ii) skeletal muscle caveolae undergo characteristic changes in size and their distribution in patients with Duchenne's muscular dystrophy, but not in other forms of muscular dystrophy examined (60). This indicates that caveolae may play an important role in muscle biology. In this regard, future studies on caveolin-3 should help to elucidate the role of caveolae in muscle cell membrane biology.

Acknowledgments—We thank the following people: Mark Chafel for confocal immunofluorescence microscopy, Guilia Baldini for help in Northern blot analysis, John R. Glenney for generously donating anti-caveolin-1 monoclonal antibodies, Tomiko Asano for purified G_{i2}, Tatsuya Haga for purified G_o, and Marcia Glatt and other members of the Whitehead purchasing department for dedicated service.

REFERENCES

1. Severs, N. J. (1988) *J. Cell Sci.* **90**, 341–348
2. Anderson, R. G. W. (1993) *Curr. Opin. Cell Biol.* **5**, 647–652
3. Simionescu, N., Simionescu, M. & Palade, G. E. (1975) *J. Cell Biol.* **64**, 586–607
4. Anderson, R. G. W., Kamen, B. A., Rothberg, K. G. & Lacey, S. W. (1992) *Science* **255**, 410–411
5. Lisanti, M. P., Scherer, P., Tang, Z.-L. & Sargiacomo, M. (1994) *Trends Cell Biol.* **4**, 231–235
6. Lisanti, M. P., Scherer, P. E., Tang, Z.-L., Kubler, E., Koleske, A. J., & Sargiacomo, M. S. (1995) *Semin. Dev. Biol.* **6**, 47–58
7. Sargiacomo, M., Sudol, M., Tang, Z.-L. & Lisanti, M. P. (1993) *J. Cell Biol.* **122**, 789–807
8. Lisanti, M. P., Scherer, P. E., Vidugiriene, J., Tang, Z.-L., Hermanoski-Vosatka, A., Tu, Y.-H., Cook, R. F. & Sargiacomo, M. (1994) *J. Cell Biol.* **126**, 111–126
9. Chun, M., Liyanage, U., Lisanti, M. P. & Lodish, H. F. (1994) *Proc. Natl. Acad. Sci. U. S. A.* **91**, 11728–11732
10. Chang, W. J., Ying, Y., Rothberg, K., Hooper, N., Turner, A., Gambliel, H., De Gunzburg, J., Mumby, S., Gilman, A. & Anderson, R. G. W. (1994) *J. Cell Biol.* **126**, 127–138
11. Shenoy-Scaria, A. M., Dietzen, D. J., Kwong, J., Link, D. C. & Lublin, D. M. (1994) *J. Cell Biol.* **126**, 353–363
12. Robbins, S. M., Quintrell, N. A. & Bishop, M. J. (1995) *Mol. Cell. Biol.* **15**, 3507–3515
13. Lisanti, M. P., Tang, Z.-L., Scherer, P. & Sargiacomo, M. (1995) *Methods Enzymol.* **250**, 655–668
14. Rothberg, K. G., Heuser, J. E., Donzell, W. C., Ying, Y., Glenney, J. R. & Anderson, R. G. W. (1992) *Cell* **68**, 673–682
15. Sargiacomo, M., Scherer, P. E., Tang, Z.-L., Kubler, E., Song, K. S., Sanders, M. C. & Lisanti, M. P. (1995) *Proc. Natl. Acad. Sci. U. S. A.* **92**, 9407–9411
16. Monier, S., Parton, R. G., Vogel, F., Behlke, J., Henske, A. & Kurzchalia, T. (1995) *Mol. Biol. Cell* **6**, 911–927
17. Li, S., Okamoto, T., Chun, M., Sargiacomo, M., Casanova, J. E., Hansen, S. H., Nishimoto, I. & Lisanti, M. P. (1995) *J. Biol. Chem.* **270**, 15693–15701
18. Corley Mastick, C., Brady, M. J. & Saltiel, A. R. (1995) *J. Cell Biol.* **129**, 1523–1531
19. Glenney, J. R. (1992) *FEBS Lett.* **314**, 45–48
20. Fan, J. Y., Carpentier, J.-L., van Obberghen, E., Grunfeld, C., Gorden, P. & Orci, L. (1983) *J. Cell Sci.* **61**, 219–230
21. Scherer, P. E., Lisanti, M. P., Baldini, G., Sargiacomo, M., Corley-Mastick, C. & Lodish, H. F. (1994) *J. Cell Biol.* **127**, 1233–1243
22. Koleske, A. J., Baltimore, D. & Lisanti, M. P. (1995) *Proc. Natl. Acad. Sci. U. S. A.* **92**, 1381–1385
23. Scherer, P. E., Tang, Z.-L., Chun, M., Sargiacomo, M., Lodish, H. F. & Lisanti, M. P. (1995) *J. Biol. Chem.* **270**, 16395–16401
24. Scherer, P. E., Okamoto, T., Chun, M., Lodish, H. F. & Lisanti, M. P. (1996) *Proc. Natl. Acad. Sci. U. S. A.* **93**, 131–135
25. Baldini, G., Hohl, T., Lin, H. & Lodish, H. F. (1992) *Proc. Natl. Acad. Sci. U. S. A.* **89**, 5049–5052
26. Tang, Z.-L., Scherer, P. E. & Lisanti, M. P. (1994) *Gene (Amst.)* **147**, 299–300
27. Cole, F., Fasy, T. M., Rao, S., de Peralta, M. & Kohtz, D. S. (1993) *J. Biol. Chem.* **268**, 1580–1585
28. Blau, H., Chiu, C.-P. & Webster, C. (1983) *Cell* **32**, 1171–1180
29. Chirgwin, J., Przybyla, R., MacDonald, R. & Rutter, W. (1979) *Biochemistry* **18**, 5294–5299
30. Sambrook, J., Fritsch, E. F. & Maniatis, T. (1989) *Molecular Cloning: A Laboratory Manual*, Cold Spring Harbor Laboratory, Cold Spring Harbor, NY
31. Kurzchalia, T., Dupree, P., Parton, R. G., Kellner, R., Virta, H., Lehnert, M. & Simons, K. (1992) *J. Cell Biol.* **118**, 1003–1014
32. Dietzen, D. J., Hastings, W. R. & Lublin, D. M. (1995) *J. Biol. Chem.* **270**, 6838–6842
33. Seed, B. & Aruffo, A. (1987) *Proc. Natl. Acad. Sci. U. S. A.* **84**, 3365–3369
34. Smart, E., Ying, Y.-S., Conrad, P. & Anderson, R. G. W. (1994) *J. Cell Biol.* **127**, 1185–1197
35. Schnitzer, J. E., Oh, P., Jacobson, B. S. & Dvorak, A. M. (1995) *Proc. Natl. Acad. Sci. U. S. A.* **92**, 1759–1763
36. Lodish, H. F. & Kong, N. (1991) *J. Biol. Chem.* **266**, 14835–14838
37. Morishita, R., Asano, T., Kato, K., Itoh, H. & Kaziro, Y. (1989) *Biochem. Biophys. Res. Commun.* **161**, 1280–1285
38. Sternweis, P. C. & Robishaw, J. D. (1984) *J. Biol. Chem.* **259**, 13806–13813
39. Okamoto, T., Katada, T., Murayama, Y., Ui, M., Ogata, E., and Nishimoto, I. (1990) *Cell* **62**, 709–717
40. Koppe, R., Hallauer, P., Karpati, G. & Hastings, K. (1989) *J. Biol. Chem.* **264**, 14327–14333
41. Sargiacomo, M., Scherer, P. E., Tang, Z.-L., Casanova, J. E. & Lisanti, M. P. (1994) *Oncogene* **9**, 2589–2595
42. Dupree, P., Parton, R. G., Raposo, G., Kurzchalia, T. V. & Simons, K. (1993) *EMBO J.* **12**, 1597–1605
43. Fra, A. M., Williamson, E., Simons, K. & Parton, R. G. (1994) *J. Biol. Chem.* **269**, 30745–30748
44. Gorodinsky, A. & Harris, D. A. (1995) *J. Cell Biol.* **129**, 619–627
45. Okamoto, T., Asano, T., Harada, S., Ogata, E. & Nishimoto, I. (1991) *J. Biol. Chem.* **266**, 1085–1091
46. Okamoto, T., Murayama, Y., Hayashi, Y., Inagaki, N., Ogata, E. & Nishimoto, I. (1991) *Cell* **67**, 723–730
47. Okamoto, T. & Nishimoto, I. (1991) *Proc. Natl. Acad. Sci. U. S. A.* **88**, 8020–8023
48. Okamoto, T. & Nishimoto, I. (1992) *J. Biol. Chem.* **267**, 8342–8346
49. Okamoto, T., Murayama, Y., Hayashi, Y., Ogata, E. & Nishimoto, I. (1993) *FEBS Lett* **334**, 143–148
50. Okamoto, T., Murayama, Y., Strittmatter, S., Katada, T., Asano, S., Ogata, E. & Nishimoto, I. (1994) *J. Biol. Chem.* **269**, 13756–13759
51. Fujimoto, T. (1993) *J. Cell Biol.* **120**, 1147–1157
52. Gabella, G. (1971) *J. Cell Sci.* **8**, 601–609
53. Gabella, G. (1989) *Anat. Embryol.* **180**, 213–226
54. Franzini-Armstrong, C., Landmesser, L. & Pilar, G. (1975) *J. Cell Biol.* **64**, 493–497
55. Zampighi, G., Vergara, J. & Ramon, F. (1975) *J. Cell Biol.* **64**, 734–740
56. Verma, V. (1984) *Eur. J. Cell Biol.* **35**, 122–128
57. Forbes, M. S., Rennels, M. & Nelson, E. (1979) *J. Ultrastruct. Res.* **67**, 325–339
58. Wolff, J. A., Dowty, M. E., Jiao, S., Repetto, G., Berg, R. K., Ludtke, J., Williams, P. & Slauterback, D. B. (1992) *J. Cell Sci.* **103**, 1249–1259
59. North, A. J., Galazkiewicz, B., Byers, T. J., Glenney, J. R. & Small, J. V. (1993) *J. Cell Biol.* **120**, 1159–1167
60. Bonilla, E., Fishbeck, K. & Schotland, D. (1981) *Am. J. Pathol.* **104**, 167–173

THE JOURNAL OF BIOLOGICAL CHEMISTRY

Vol. 272, No. 28, Issue of July 11, pp. 17744–17748, 1997
Printed in U.S.A.

Dynamic Targeting of the Agonist-stimulated m2 Muscarinic Acetylcholine Receptor to Caveolae in Cardiac Myocytes*

(Received for publication, April 3, 1997, and in revised form, May 1, 1997)

Olivier Feron‡, Thomas W. Smith, Thomas Michel§, and Ralph A. Kelly¶

From the Cardiovascular Division, Department of Medicine, Brigham and Women's Hospital and Harvard Medical School, Boston, Massachusetts 02115

In cardiac myocytes, as well as specialized conduction and pacemaker cells, agonist binding to muscarinic acetylcholine receptors (mAchRs) results in the activation of several signal transduction cascades including the endothelial isoform of nitric-oxide synthase (eNOS) expressed in these cells. Recent evidence indicates that, as in endothelial cells, eNOS in cardiac myocytes is localized to plasmalemma caveolae, specialized lipid microdomains that contain caveolin-3, a muscle-specific isoform of the scaffolding protein caveolin. In this report, using a detergent-free method for isolation of sarcolemmal caveolae from primary cultures of adult rat ventricular myocytes, we demonstrated that the muscarinic cholinergic agonist carbachol promotes the translocation of mAchR into low density gradient fractions containing most myocyte caveolin-3 and eNOS. Following isopycnic centrifugation, the different gradient fractions were exposed to the muscarinic radioligand [^{3}H]quinuclidinyl benzilate (QNB), and binding was determined after membrane filtration or immunoprecipitation. In a direct radioligand binding assay, we found that [^{3}H]QNB binding can be detected in caveolin-enriched fractions only when cardiac myocytes have been previously exposed to carbachol. Furthermore, most of this [^{3}H]QNB binding can be specifically immunoprecipitated by an antibody to the m2 mAchR, indicating that the translocation of this receptor subtype is responsible for the [^{3}H]QNB binding detected in the low density fractions. Moreover, the [^{3}H]QNB binding could be quantitatively immunoprecipitated from the light membrane fractions with a caveolin-3 antibody (but not a control IgG1 antibody), confirming that the m2 mAchR is targeted to caveolae after carbachol treatment. Importantly, atropine, a muscarinic cholinergic antagonist, did not induce translocation of m2 mAchR to caveolae and prevented receptor translocation in response to the agonist carbachol. Thus, dynamic targeting of sarcolemmal m2 mAchR to caveolae following agonist binding may be essential to initiate specific downstream signaling cascades in these cells.

The activation of a muscarinic acetylcholine receptor (mAChR)[1] triggers a number of signal transduction pathways that, in the heart, may elicit both positively and negatively inotropic and chronotropic effects (1, 2). Recent studies have shown that, of the five mAchR subtypes identified to date, only the m1 and m2 subtypes are expressed in adult mammalian cardiac tissues (3, 4). According to these reports, the m2 mAchR, which is expressed at a much higher level than the m1 mAchR, triggers the inhibitory response while m1 receptor activation elicits, when stimulated by higher concentrations of agonist, a compensatory excitatory effect on heart function. Therefore, distinct downstream signaling cascades must be involved following m1 and m2 mAchR activation. Both m1 and m2 receptor subtypes also have been reported to undergo translocation into specific subcompartments derived from the plasma membrane (5–10), a characteristic of many G protein-coupled receptors (GPR) following agonist binding. To date, two major pathways for GPR clustering and sequestration have been reported, which involve plasma membrane modifications that lead to the formation of either clathrin-coated or non-coated vesicles (11). While the human muscarinic cholinergic receptor Hm1 has been shown to internalize via clathrin-coated vesicles (10), mAchR have also been shown to be internalized through non-clathrin-coated vesicles in human fibroblasts, although the identity of these vesicular structures has not been defined (6).

Recently, a clathrin-independent sequestration pathway has received attention with the characterization of a population of plasmalemmal vesicles termed caveolae. Caveolae are small flask-shaped invaginations of the plasma membrane characterized by high levels of cholesterol and glycosphingolipids (12), the principal scaffolding protein of which are the caveolins, 20–24 kDa integral membrane proteins that undergo homo-oligomerization (13). These specialized lipid microdomains have been shown to play a role in the compartmentation of a number of plasma membrane-linked signal transduction pathways, including those mediated by receptor tyrosine kinases (14, 15). In addition, a recent report by Parton *et al.* (16) provides additional evidence that coalescence and fission of caveolae may be essential for the development of the T-tubular system that is essential for normal intracellular calcium homeostasis and excitation-contraction coupling in cardiac and skeletal muscle. The specific mechanisms involved in receptor sequestration may differ among distinct cellular phenotypes. For example, several reports have proposed the involvement of

* This work was supported by National Institutes of Health Grant HL-52320 (to T. W. S.). The costs of publication of this article were defrayed in part by the payment of page charges. This article must therefore be hereby marked "*advertisement*" in accordance with 18 U.S.C. Section 1734 solely to indicate this fact.

‡ Recipient of a fellowship from the Belgian American Educational Foundation and of a grant from the "Patrimoine Facultaire de l'UCL" (Belgium).

§ A Wyeth-Ayerst Established Investigator of the American Heart Association and recipient of a Scholar Award in Experimental Therapeutics from the Burroughs-Wellcome Fund.

¶ To whom correspondence should be addressed: Cardiovascular Div., Brigham and Women's Hospital, Harvard Medical School, 75 Francis St., Boston, MA 02115. Tel.: 617-732-7503; Fax: 617-732-5132; E-mail: rakelly@bics.bwh.harvard.edu or michel@calvin.bwh.harvard.edu.

[1] The abbreviations used are: mAchR, muscarinic acetylcholine receptor(s); GPR, G protein-coupled receptor; β-AR, β-adrenergic receptor; eNOS, endothelial isoform of nitric-oxide synthase; NO, nitric oxide; ARVM, adult rat ventricular myocytes; QNB, 1-quinuclidinyl benzilate; CHAPS, 3-[(3-cholamidopropyl)dimethylammonio]-1-propanesulfonic acid; Mes, 4-morpholineethanesulfonic acid; MBS, Mes-buffered saline; PVDF, polyvinylidene difluoride; TBST, Tris-buffered saline with Tween 20; PAGE, polyacrylamide gel electrophoresis.

clathrin-coated pits in the mechanism of internalization of β-adrenergic receptors (β-AR) (17), and yet a recent report indicated that in epidermoid A431 cells, β-AR are clustered within caveolae in response to agonist stimulation (18).

The recent development of antibodies directed against different tissue-specific isoforms of caveolin has permitted a better characterization of caveolar microdomains. Using these antibodies in immunoprecipitation experiments, we have recently shown that eNOS, the constitutively expressed isoform of nitric-oxide synthase in cardiac myocytes, is targeted to sarcolemmal caveolae in cardiac myocytes and endothelial cells (19). Interestingly, reports from our laboratory and by others have shown that the generation of nitric oxide (NO) is an obligate intermediate step in the signal transduction cascade involved in the m2 mAchR-mediated inhibitory responses of the heart, particularly following β-adrenergic stimulation (20–23). Caveolae may, therefore, constitute the structural framework within which this signaling cascade operates. Thus, the dynamic targeting of agonist-stimulated muscarinic cholinergic receptors to caveolae in cardiac myocytes could facilitate the activation of eNOS, which we have shown to be quantitatively and specifically associated with caveolin-3, the muscle-specific isoform of caveolin (19, 24–26). The co-localization in caveolae of this Ca^{2+}/calmodulin-dependent NOS isoform with proteins known to regulate Ca^{2+} homeostasis, including a Ca^{2+}-ATPase and $InsP_3$ receptor-like proteins (27), as well as with heterotrimeric G proteins (12, 26, 28), suggest that these plasmalemmal microdomains may constitute a platform for the recruitment and regulation of the signaling proteins involved in the NO-mediated muscarinic cholinergic pathway in heart muscle.

In this report, we describe experiments designed to explore the hypothesis that m2 mAchR are targeted to plasmalemmal caveolae upon agonist stimulation in adult rat ventricular myocytes. Using a detergent-free method for caveolae isolation followed by isopycnic centrifugation, we provide evidence that the m2 mAchR, after agonist stimulation, co-purifies with caveolin-3 and eNOS. Furthermore, we show that the radioliganded m2 mAchR can be specifically immunoprecipitated from these caveolin-enriched fractions using antibodies directed against caveolin-3.

EXPERIMENTAL PROCEDURES

Cell Culture, Lysate Preparation, and Subfractionation—Purified adult rat ventricular myocyte (ARVM) primary cultures were plated on laminin and cultured for 24 h in a defined medium as reported previously (19). ARVM were incubated either with or without carbachol (100 μM, 15 min), lysed, and fractionated on sucrose gradients; in some experiments (see "Results and Discussion"), myocytes were preincubated in the presence of 1 μM atropine (15 min) or 5 mM acetic acid (5 min) before carbachol treatment. Before harvesting, cells were washed extensively with ice-cold phosphate-buffered saline to ensure complete removal of drugs. This was validated by the lack of any detectable difference in specific [^{3}H]quinuclidinyl benzylate (QNB) binding levels (see below) in total lysates of ARVM, whether treated or not with a muscarinic agonist or antagonist.

ARVM were scraped in a freshly prepared solution of 200 mM Na_2CO_3 and lysed by sonication (three 5-s bursts, minimal output power) using a Branson sonifier 450 (Branson Ultrasonic Corp., Danbury, CT), according to a method modified from Song *et al.* (26). The cell lysate was then adjusted to 45% sucrose by addition of a sucrose stock solution prepared in MBS (25 mM Mes, pH 6.5, 150 mM NaCl) and placed at the bottom of a 5–15-25–35% discontinuous sucrose gradient (in MBS containing 100 mM Na_2CO_3) for an overnight ultracentrifugation (150,000 g). The gradient was fractionated in nine fractions corresponding to sucrose concentrations 5, 15, 25, 35, and 45%, and the four intermediate interfaces. Each fraction was neutralized with HCl before further analysis.

SDS-PAGE and Immunoblotting—Heat-denatured proteins were loaded and separated on 12% SDS-polyacrylamide gels (Mini Protean II, Bio-Rad) and transferred to a PVDF membrane (Bio-Rad). After blocking with 5% non-fat dry milk in Tris-buffered saline with 0.1% (v/v) Tween 20 (TBST), membranes were incubated with the specified primary antibody (Transduction Labs) for 1 h in TBST containing 1% non-fat dry milk. After six washes (10 min each), the membranes were incubated for 1 h with a horseradish peroxidase-labeled goat anti-mouse immunoglobulin secondary antibody (Jackson ImmunoResearch Labs) at a 1:10,000 dilution in TBST containing 1% non-fat dry milk. After five additional washes, the membranes were rinsed once in TBST, incubated with a chemiluminescent reagent according to the manufacturer protocols (Renaissance, NEN Life Science Products), and exposed to x-ray film.

Membrane Markers—Mannosidase II activity was determined by hydrolysis of *p*-nitrophenyl-α-D-mannopyranoside (Sigma) with volumes reduced to facilitate the assay in 96-well plates, as described previously (29). After incubation at 37 °C for 1 h followed by quenching with 100 mM NaOH, absorbance was measured at 405 nm using a Microplate Reader (SLT Lab Instruments). [^{3}H]ouabain (NEN Life Science Products) binding was determined as described (30); nonspecific binding was estimated in the presence of 1 mM ouabain (Sigma). Membranes were collected on Whatman GF/B fiber filters, washed twice with chilled Tris-HCl, pH 7.4, and the radioactivity was determined in a scintillation counter. Protein amounts, mannosidase activity and [^{3}H]ouabain binding are expressed as percent of total protein, of total activity, and of total specific [^{3}H]ouabain binding, respectively.

Radioligand Experiments and Immunoprecipitation—The gradient fractions (buffered at pH 7.4) were adjusted to 5 mM $MgCl_2$, 1 mM EGTA, 1 μg/ml leupeptin, 1 μg/ml pepstatin, and 1 mM phenylmethylsulfonyl fluoride, and aliquots of the different fractions were incubated with 2 nM [^{3}H]QNB (NEN Life Science Products) at 30 °C for 60 min; nonspecific binding was determined in the presence of 1 μM atropine. Assays were performed in triplicate and terminated by rapid filtration on Whatman GF/B filters or followed by an immunoprecipitation protocol (adapted from those in Refs. 31 and 32). For these immunoprecipitation experiments, the binding buffer also contained 1% digitonin and 0.2% CHAPS; nonspecific [^{3}H]QNB binding was determined by performing all the steps of the immunoprecipitation protocol in the presence of 1 μM atropine. After sequential incubations of the [^{3}H]QNB-bound receptors with an antibody directed against the m2 mAchR (4 h, 4 °C, Chemicon) and agarose-conjugated protein-G (1–2 h, 4 °C), immunocomplexes were precipitated by centrifugation, washed four times with 25 mM Mes buffer containing 1% digitonin and 0.2% CHAPS, and resuspended in 1% SDS. A similar protocol was used for the immunoprecipitation with the caveolin-3 antibody (Transduction Labs) except that binding and washing buffers did not contain digitonin. The isoform specificity and lack of cross-reactivity of the caveolin (19, 24–26) and muscarinic (32) antibodies have been established previously. Moreover, the specificity of the caveolin-3 immunoprecipitation was established by comparing the [^{3}H]QNB binding detected from immunoprecipitates performed using a non-immune idiotype-specific purified mouse myeloma IgG1 (Zymed). In all the experiments described here above, samples were transferred in counting vials containing 10 ml of scintillant, and the radioactivity was determined in a liquid scintillation counter.

RESULTS AND DISCUSSION

Caveolae Isolation by Subcellular Fractionation of Cardiac Myocytes—Caveolin-enriched membranes have been historically isolated on the basis of their insolubility in Triton due to their specialized lipid composition (12, 33). However, it has been reported recently that the inclusion of detergent can result in the loss of proteins normally associated with caveolae (26, 34), as well as in apparent redistribution of mitochondrial and endoplasmic reticulum proteins into caveolae (35). Therefore, for isolating caveolae from cardiac myocytes, we have optimized a detergent-free purification method based on the resistance to extraction of caveolin complexes by sodium carbonate and on the fine disruption of cellular membrane by sonication (18, 26). Thus, after homogenization of ARVM in a sodium carbonate buffer, the lysate was adjusted to 45% sucrose and placed at the bottom of a 5–15-25–35% discontinuous gradient for an overnight ultracentrifugation. Aliquots of the different fractions collected were separated by SDS-PAGE, transferred onto PVDF membranes, and immunoblotted with anti-caveolin-3 or anti-eNOS antibodies. The immunoblots presented in Fig. 1*A* show that the majority of caveolin-3 and

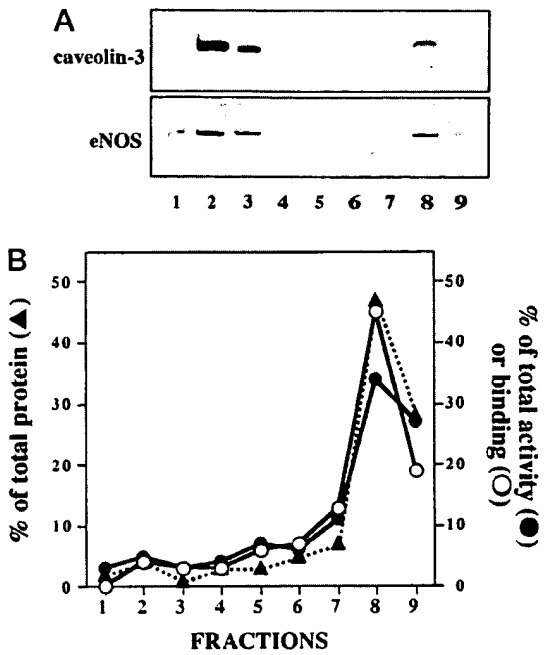

FIG. 1. **Fractionation of cardiac myocytes.** *A*, distribution of caveolin-3 and eNOS proteins. After isopycnic centrifugation of adult rat ventricular myocytes on sucrose gradients as described in the text, aliquots of 1 ml-fractions were resolved by SDS-PAGE (12.5% acrylamide), transferred onto PVDF membranes, and immunoblotted with an anti-caveolin-3 antibody or eNOS antibody. Fraction 1 refers to the top of the gradient. These data represent the result of a typical fractionation experiment. *B*, distribution of protein (▲), plasma membrane (○), and Golgi (●) markers along sucrose density gradient. The mannosidase II activity and the [^{3}H]ouabain binding have been used as specific markers of the Golgi and the plasma membrane, respectively. Fraction 1 refers to the top of the gradient. The data represent the results of typical fractionation procedures with individual measurements performed in triplicate.

eNOS in ventricular myocytes appears in fractions 2 and 3, which correspond to the 5–15% sucrose equilibrium densities. This co-purification of eNOS and caveolin-3 is in agreement with our previous data on the co-immunoprecipitation of these two proteins from CHAPS-solubilized cardiac myocyte lysates (19) and on the co-isolation of eNOS and caveolin-1 in endothelial cells (36).

The gradient fractions were also analyzed for their protein content as well as for the presence of mannosidase II, as a Golgi marker (29), and for the level of specific [^{3}H]ouabain binding (30), as a specific marker of (Na^+, K^+)-ATPase, a relatively evenly distributed enzyme at the sarcolemmal surface of cardiac myocytes. As shown by the pattern of distribution of these markers across the gradient (Fig. 1*B*), the bulk of cellular protein that equilibrates at the high sucrose density (fractions 7–9), corresponds to Golgi and sarcolemmal membranes. The small amount of caveolin-3 and eNOS associated with these high density fractions (Fig. 1*A*) is probably due to some association of both proteins with the trans-Golgi network (37) or to incomplete cell lysis prior to sucrose density gradient centrifugation.

Agonist-induced Targeting of Muscarinic Cholinergic Receptor to Caveolin-enriched Fractions—We next explored the effects of carbachol, a muscarinic cholinergic agonist, on the distribution of mAchR using the centrifugation protocol described above, to determine if a change in receptor subcellular localization was induced by agonist binding. The following experiments were performed on primary cultures of ARVM exposed to 100 μM carbachol for 15 min. After extensive washing, myocytes were lysed and submitted to isopycnic centrifugation on a sucrose gradient. Aliquots of the different fractions obtained were incubated with [^{3}H]QNB, a muscarinic antagonist radioligand, at 30 °C for 60 min. In a first set of experiments, membranes were directly filtered on Whatman GF/B glass filters. As shown in Fig. 2*A*, in lysates prepared from untreated myocytes, the binding of [^{3}H]QNB is only detected in the high-density fractions. In contrast, following carbachol treatment, 27.4 ± 3.3% of the [^{3}H]QNB binding (n = 6) can be recovered in the low-density fractions 2 and 3, which correspond to the caveolin-enriched membranes (Fig. 1*A*). The rest of the [^{3}H]QNB binding remains concentrated in fractions 7–9 and likely represents binding to non-caveolar sarcolemmal muscarinic receptors.

In a second series of experiments, we used a complementary approach to explore the carbachol-induced shift in [^{3}H]QNB binding. The different fractions collected after isopycnic centrifugation were immunoprecipitated using an m2 mAchR antibody, and the amount of specific [^{3}H]QNB binding in each immunoprecipitate was determined. As shown in Fig. 2*B*, the pattern of distribution of m2 mAchR is similar to that directly deduced from the [^{3}H]QNB binding to each fraction (Fig. 2*A*) with, however, a more accentuated shift of [^{3}H]QNB bound m2 mAchR toward the low density fractions when myocytes have been exposed to carbachol. 34.6 ± 3.9% (n = 6) of the [^{3}H]QNB binding is now detected in the caveolar fractions 2 and 3. Importantly, when ARVM are preincubated with 1 μM atropine before carbachol treatment (Fig. 2*C*), the enrichment of the m2 mAchR in fractions 2 and 3 is no longer observed, thereby indicating the specificity of the agonist-mediated clustering process. Interestingly, in a previous study, Raposo *et al.* (6) reported that treatment of human fibroblasts, either with a muscarinic cholinergic agonist or with the muscarinic cholinergic antagonist atropine, triggered the redistribution of the Hm1 mAchR into specific regions of the plasma membrane, presumably caveolae, and that only longer exposures with the agonist lead to the receptor endocytosis. Furthermore, Tolbert and Lameh (10) showed, using immunofluorescence confocal microscopy, that the Hm1 mAchR, after agonist stimulation, are internalized via clathrin-coated vesicles in HEK cells stably transfected with the epitope-tagged Hm1 receptors. Together with the data reported here, these results suggest that the extent and the mode of receptor compartmentation in response to agonist stimulation may be governed by both the receptor subtype and the cell type in which it is expressed.

In our experimental conditions, it is unlikely that clustering of the m2 mAchR into coated pits can explain the shift in mAchR into lower density sucrose gradients. Indeed, evidence from the literature indicates that the equilibrium density of clathrin-coated pits is higher than that of caveolae (38) and therefore would not match the pattern of distribution of carbachol-stimulated muscarinic receptors obtained in Fig. 2, *A* and *B*. Furthermore, when myocytes are pre-incubated with 5 mM acetic acid, pH 5.0, a treatment known to disrupt clathrin-mediated endocytosis (39), a movement of m2 mAchR into caveolin-enriched fractions is still detected (Fig. 2*C*).

Immunoprecipitation by Caveolin-3 Antibody of Agonist-stimulated Muscarinic Cholinergic Receptors—To confirm the dynamic targeting of muscarinic receptors to caveolae in cardiac myocytes, we used a caveolin-3 antibody to immunoprecipitate caveolar membranes and identify the m2 mAchR by radioligand binding assays. In these studies, cardiac myocytes preincubated either with or without carbachol were lysed and fractionated on sucrose gradients, and the fractions corresponding to caveolae were pooled and incubated with [^{3}H]QNB. After subsequent incubation with either an anti-caveolin-3 an-

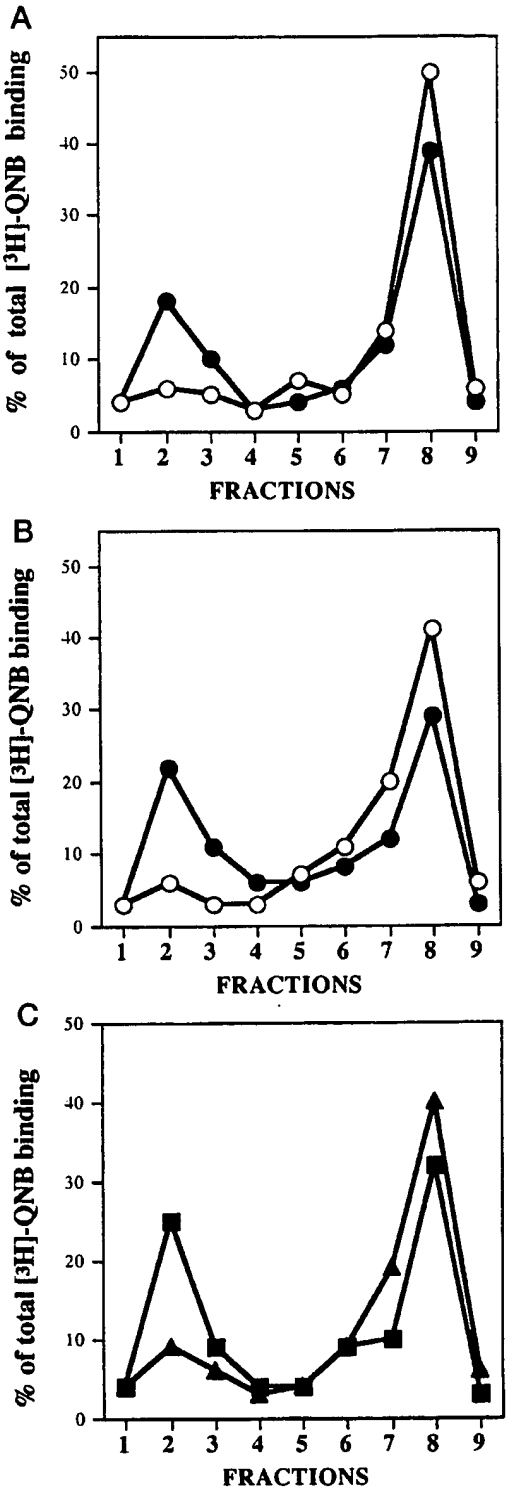

FIG. 2. **Agonist-induced translocation of muscarinic receptors in cardiac myocytes.** The presence of muscarinic receptors in each fraction is determined by the amount of specific [^{3}H]QNB binding detected by harvesting membranes on Whatman glass filters (*A*) or by immunoprecipitation with anti-m2 antibodies (*B, C*); control and carbachol (100 μM, 15 min) conditions are symbolized by open (○) and closed (●, ▲, ■) symbols, respectively. In panel *C*, the incubation in presence of carbachol (100 μM, 15 min) was preceded by a 15-min incubation with atropine 1 μM (▲) or a 5-min incubation with 5 mM acetic acid, pH 5.0 (■). For each condition, nonspecific binding was determined in the presence of 1 μM atropine. The data are expressed as the percent of total specific [^{3}H]QNB binding and are representative of those obtained in three to six experiments.

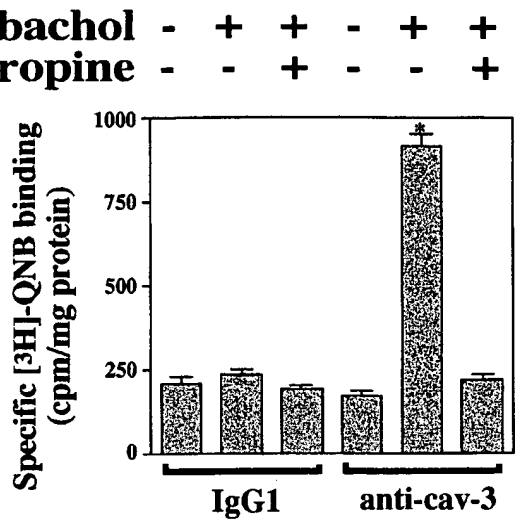

FIG. 3. **Caveolin-immunoprecipitation of agonist-stimulated muscarinic receptors.** Low density caveolin-enriched fractions (fractions 2 and 3, see Fig. 1) isolated from cardiac myocytes pretreated with or without carbachol (100 μM, 15 min) were incubated with [^{3}H]QNB at 30 °C for 30 min and immunoprecipitated using an anti-caveolin-3 or nonspecific IgG1 antibody. Total and nonspecific [^{3}H]QNB binding were determined by performing immunoprecipitations in the absence or presence of 1 μM atropine. The results represent the specific [^{3}H]QNB binding (± S.E., n = 3–5; *, $p < 0.01$ *versus* all other conditions) determined from each immunoprecipitation and are expressed as cpm/mg of protein.

tibody or a nonspecific IgG1 antibody and agarose-conjugated protein-G, immunocomplexes were collected by centrifugation, and radioactivity was determined in a scintillation counter.

As summarized in Fig. 3, in the absence of carbachol treatment, there was no significant immunoprecipitation of [^{3}H]QNB binding by caveolin-3 antibodies since the level of [^{3}H]QNB binding was similar to that obtained when using the nonspecific IgG1 for the immunoprecipitation. In contrast, following agonist treatment, a substantial fraction of specific [^{3}H]QNB binding can be immunoprecipitated by anti-caveolin-3 antibodies (Fig. 3); no change in caveolin-3 expression was observed after carbachol treatment (not shown). In fact, 73 ± 5% (n = 3) of the [^{3}H]QNB binding originally present in pooled fractions 2 and 3 (determined by direct filtration on Whatman GF/B glass filters) could be recovered after anti-caveolin-3 immunoprecipitation. Similar experiments (not shown) performed on fractions 7–9, which correspond to the bulk of plasma membrane (80–95% of total protein when pooled together), did not reveal any specific [^{3}H]QNB binding in the caveolin-3 immunoprecipitate, in agreement with the low abundance of caveolin-3 in these fractions (see Fig. 1*A*). Importantly, in myocytes incubated with carbachol in the presence of the muscarinic antagonist atropine, the [^{3}H]QNB binding immunoprecipitated by anti-caveolin-3 antibodies remained at the level detected in a control immunoprecipitation performed with a nonspecific IgG1. This is in agreement with the data shown in Fig. 2*C* in which no significant binding was detected in the anti-m2 mAchR immunoprecipitates from caveolar fractions of myocytes incubated with carbachol in the presence of atropine. Taken together, these data establish that the m2 mAchR redistributes to plasmalemmal caveolae of cardiac myocytes following agonist binding.

The dynamic targeting of the m2 mAchR to caveolae has important implications for muscarinic receptor biology as well as for the regulation of eNOS activation. Although several laboratories have reported evidence for the translocation to low density gradient fractions of the muscarinic receptors upon

agonist stimulation (5–7), there are, to our knowledge, no data in the literature that address the specific nature of these "light membranes." The co-purification and co-immunoprecipitation (this study, and also see Refs. 19 and 36) of caveolin, eNOS, and the agonist-stimulated m2 mAchR in isopycnic centrifugation fractions, which together represent less than 5% of the total amount of protein, indicate that caveolae are the common structural platform for these proteins. Together with immunoelectron microscopy data showing that, in A431 cells, β-AR are sequestrated within caveolae in response to agonist stimulation (18), our data indicate that clathrin-coated pit formation can no longer be considered as the exclusive pathway for clustering G protein-coupled receptors within specialized plasmalemmal microdomains. The fate of caveolar β-AR and mAchR is uncertain, since it is not clear whether caveolae pinch off from the plasma membrane and lead to early endosomes. If this is the case, it suggests that dual pathways of receptor internalization may exist in some cells.

While numerous studies present the sequestration of G protein-coupled receptors after agonist stimulation as a key event for initiating a process of desensitization (for review, see Ref. 40), the data in this manuscript support the hypothesis that, following stimulation by agonist, cardiac m2 mAchR translocation to caveolae may be necessary to initiate specific downstream signaling cascades. Interestingly, several recent studies have shown that internalization of the m2 and m4 mAchR is mediated by mechanisms distinct from the phosphorylation by the G protein-coupled receptor kinase (GRK) family known to lead to receptor desensitization (41, 42). The translocation of muscarinic receptors within caveolae should allow their interaction with the heterotrimeric G protein complexes known to be concentrated within these plasmalemmal microdomains (12, 26, 28) and lead, after recruitment of co-factors and intermediate effector proteins, to the activation of eNOS, a resident caveolar protein in cardiac myocytes. Analysis of caveolin-enriched fractions to identify additional signaling molecules involved in the muscarinic cholinergic stimulation of the NO pathway in cardiac myocytes is ongoing in our laboratory. The caveolar compartmentation described here for the muscarinic cholinergic pathway may serve as a paradigm for other G protein receptor-mediated signaling cascades that are targeted to caveolae.

REFERENCES

1. Korth, M., and Kühlkamp, V. (1985) *Pfluegers Arch. Eur. J. Physiol.* **403,** 266–272
2. Eglen, R. M., Montgomery, W. W., and Whiting, R. L. (1988) *J. Pharmacol. Exp. Ther.* **247,** 911–917
3. Gallo, M. P., Alloatti, G., Eva, C., Oberto, A., and Levi. R. C. (1993) *J. Physiol.* **471,** 41–60
4. Sharma, V. K., Colecraft, H. M., Wang, D. X., Levey, A. I., Grigorenko, E. V., Yeh, H. H., and Sheu, S.-S. (1996) *Circ. Res.* **79,** 86–93
5. Harden, T. K., Petch, L. A., Traynelis, S. F., and Waldo, G. L. (1985) *J. Biol. Chem.* **260,** 13060–13066
6. Raposo, G., Dunia, I., Marullo, S., André, Guillet, J.-G., Strosberg, A. D., Benedetti, E. L., and Hoebeke, J. (1987) *Biol. Cell* **60,** 117–124
7. Ho, A. K. S., Zhang, Y.-J., Duffield, R., and Zheng, G.-M. (1991) *Cell. Signalling* **3,** 587–598
8. Svoboda, P., and Milligan, G. (1994) *Eur. J. Biochem.* **224,** 455–462
9. Goldman, P. S., Schlador, M. L., Shapiro, R. A., and Nathanson, N. M. (1996) *J. Biol. Chem.* **271,** 4215–4222
10. Tolbert, L. M., and Lameh, J. (1996) *J. Biol. Chem.* **271,** 17335–17342
11. Sandvig, K., and van Deurs, B. (1994) *Trends Cell Biol.* **4,** 275–277
12. Sargiacomo, M., Sudol, M., Tang, Z., and Lisanti, M. P. (1993) *J. Cell Biol.* **122,** 789–807
13. Monier, S., Parton, R. G., Vogel, F., Behlke, J., Henske, A., and Kurzchalia, T. V. (1995) *Mol. Biol. Cell* **6,** 911–927
14. Liu, P., Ying, Y., Ko, Y.-G., and Anderson, R.'G. W. (1996) *J. Biol. Chem.* **271,** 10299–10303
15. Mineo, C., James, G. L., Smart, E. J., and Anderson, R. G. W. (1996) *J. Biol. Chem.* **271,** 11930–11935
16. Parton, R. G., Way, M., Zorzi, N., and Stang, E. (1997) *J. Cell Biol.* **136,** 137–154
17. Muntz, K. H. (1994) *Trends Cell Biol.* **6,** 356
18. Dupree, P., Parton, R. G., Raposo, G., Kurzhalia, T. V., and Simons, K. (1993) *EMBO J.* **12,** 1597–1605
19. Feron, O., Belhassen, L., Kobzik, L., Smith, T. W., Kelly, R. A., and Michel, T. (1996) *J. Biol. Chem.* **271,** 22810–22814
20. Balligand, J.-L., Kelly, R. A., Marsden, P. A., Smith, T. W., and Michel, T. (1993) *Proc. Natl. Acad. Sci. U. S. A.* **90,** 347–351
21. Balligand, J.-L., Kobzik, L., Han, X., Kaye, D. M., Belhassen, L., O'Hara, D. S., Kelly, R. A., Smith, T. W., and Michel, T. (1995) *J. Biol. Chem.* **270,** 14582–14586
22. Han, X., Shimoni, Y., and Giles, W. R. (1995) *J. Gen. Physiol.* **106,** 45–65
23. Han, X., Kobzik, L., Balligand, J.-L., Kelly, R. A., and Smith, T. W. (1996) *Circ. Res.* **78,** 998–1008
24. Way, M., and Parton, R. G. (1996) *FEBS Lett.* **378,** 108–112
25. Tang, Z., Scherer, P. E., Okamoto, T., Song, K., Chu, C., Kohtz, D. S., Nishimoto, I., Lodish, H. F., and Lisanti, M. P. (1996) *J. Biol. Chem.* **271,** 2255–2261
26. Song, K. S., Li, S., Okamoto, T., Quilliam, L. A., Sargiacomo, M., Lisanti, M. P. (1996) *J. Biol. Chem.* **271,** 9690–9697
27. Fujimoto, T. (1993) *J. Cell Biol.* **120,** 1147–1157
28. Schnitzer, J. E., Liu, J., and Oh, P. (1995) *J. Biol. Chem.* **270,** 14399–14404
29. Denker, S. P., McCaffery, J. M., Palade, G. E., Insel, P. A., and Farquhar, M. G. (1996) *J. Cell Biol.* **133,** 1027–1040
30. Feron, O., Wibo, M., Christen, M.-O., and Godfraind, T. (1992) *Br. J. Pharmacol.* **105,** 480–484
31. Luthin, G. R., Harkness, J., Artymyshyn, R. P., and Wolfe, B. B. (1988) *Mol. Pharmacol.* **34,** 327–333
32. Levey, A. I., Kitt, C. A., Simonds, W. F., Price, D. L., and Brann, M. R. (1991) *J. Neurosci.* **11,** 3218–3226
33. Parton, R. G. (1996) *Curr. Opin. Cell Biol.* **8,** 542–548
34. Smart, E. J., Ying, Y.-S., Mineo, C., and Anderson, R. G. W. (1995) *Proc. Natl. Acad. Sci. U. S. A.* **92,** 10104–10108
35. Kurzchalia, T. V., Hartmann, E., and Dupree, P. (1995) *Trends Cell Biol.* **5,** 187–189
36. Shaul, P. W., Smart, E. J., Robinson, L. J., German, Z., Yuhanna, I. S., Ying, Y., Anderson, R. G. W., and Michel, T. (1996) *J. Biol. Chem.* **271,** 6518–6522
37. Belhassen, L., Feron, O., Kaye, D. M., Michel, T., Smith, T. W., and Kelly, R. A. (1997) *J. Biol. Chem.* **272,** 11198–11204
38. Woodward, M. P., and Roth, T. F. (1978) *Proc. Natl. Acad. Sci. U. S. A.* **75,** 4394–4398
39. Sandvig., K., Olsnes, S., Petersen, O. W., and Deurs, B. V. (1987) *J. Cell Biol.* **105,** 679–689
40. Eva, C., Gamalero, S. R., Genazzani, E., and Costa, E. (1990) *J. Pharmacol. Exp. Therap.* **253,** 257–265
41. Pals-Rylaarsdam, R., Xu, Y., Witt-Enderby, P., Benovic, J. L., and Hosey, M. M. (1995) *J. Biol. Chem.* **270,** 29004–29011
42. Bogatkewitsch, G. S., Lenz, W., Jakobs, K. H., and van Koppen, C. J. (1996) *Mol. Pharmacol.* **50,** 424–429

THE JOURNAL OF BIOLOGICAL CHEMISTRY Vol. 272, No. 46, Issue of November 14, pp. 29337–29346, 1997

Printed in U.S.A.

Cell-type and Tissue-specific Expression of Caveolin-2

CAVEOLINS 1 AND 2 CO-LOCALIZE AND FORM A STABLE HETERO-OLIGOMERIC COMPLEX *IN VIVO**

(Received for publication, August 6, 1997, and in revised form, September 10, 1997)

Philipp E. Scherer‡, Renée Y. Lewis‡, Daniela Volonté§¶, Jeffrey A. Engelman§¶, Ferruccio Galbiati§¶, Jacques Couet‖, D. Stave Kohtz, Elly van Donselaar‡‡, Peter Peters‡‡, and Michael P. Lisanti§ §§**

*From the Departments of ‡Cell Biology and §Molecular Pharmacology, Albert Einstein College of Medicine, Bronx, New York 10461, the ‖Laval Hospital Research Center, Sainte-Foy, Quebec, Canada, the **Mount Sinai School of Medicine, Department of Pathology, New York, New York 10029, and the ‡‡Faculty of Medicine, Cell Biology, Heidelberglaan100 - H02., 3143584 CX Utrecht, The Netherlands*

Caveolae are microdomains of the plasma membrane that have been implicated in organizing and compartmentalizing signal transducing molecules. Caveolin, a 21–24-kDa integral membrane protein, is a principal structural component of caveolae membrane *in vivo*. Recently, we and other laboratories have identified a family of caveolin-related proteins; caveolin has been retermed caveolin-1.

Here, we examine the cell-type and tissue-specific expression of caveolin-2. For this purpose, we generated a novel mono-specific monoclonal antibody probe that recognizes only caveolin-2, but not caveolins-1 and -3. A survey of cell and tissue types demonstrates that the caveolin-2 protein is most abundantly expressed in endothelial cells, smooth muscle cells, skeletal myoblasts (L6, BC3H1, C2C12), fibroblasts, and 3T3-L1 cells differentiated to adipocytes. This pattern of caveolin-2 protein expression most closely resembles the cellular distribution of caveolin-1. In line with these observations, co-immunoprecipitation experiments with mono-specific antibodies directed against either caveolin-1 or caveolin-2 directly show that these molecules form a stable hetero-oligomeric complex. The *in vivo* relevance of this complex was further revealed by dual-labeling studies employing confocal laser scanning fluorescence microscopy. Our results indicate that caveolins 1 and 2 are strictly co-localized within the plasma membrane and other internal cellular membranes. Ultrastructurally, this pattern of caveolin-2 localization corresponds to caveolae membranes as seen by immunoelectron microscopy. Despite this strict co-localization, it appears that regulation of caveolin-2 expression occurs independently of the expression of either caveolin-1 or caveolin-3 as observed using two different model cell systems. Although caveolin-1 expression is down-regulated in response to oncogenic transformation of NIH 3T3 cells, caveolin-2 protein levels remain unchanged. Also, caveolin-2 protein levels remain unchanged during the differentiation of C2C12 cells from myoblasts to myotubes, while caveolin-3 levels are dramatically induced by this process. These results suggest that expression levels of caveolins 1, 2, and 3 can be independently up-regulated or down-regulated in response to a variety of distinct cellular cues.

Caveolae are small omega-shaped indentations of the plasma membrane that have been implicated in signal transduction and vesicular transport processes (1, 2). Caveolae are found in most cell types but are extremely abundant in terminally differentiated cell types: adipocytes (3–5), simple squamous epithelia (type I pneumocytes and endothelial cells) (6), smooth muscle cells (7), and fibroblasts (8). Caveolin, a 21–24-kDa integral membrane protein, is a principal structural component of caveolae membranes *in vivo* (9–13).

Several independent lines of evidence suggest that caveolin functions as a scaffolding protein within caveolae membranes. Caveolin forms a high molecular mass oligomeric complex (14, 15) that is thought to represent the assembly unit of caveolae membranes (16), and recombinant expression of caveolin in caveolin-negative cells is sufficient to drive the formation of caveolae-sized vesicles (17–19). As caveolin interacts directly with cholesterol (20, 21) and glyco-sphingolipids (22), it has been proposed that the caveolin-mediated selection of endogenous lipid components could provide the driving force for caveolae formation (18).

Loss or dramatic reduction of caveolin expression and caveolae occurs in NIH 3T3 cells transformed by activated oncogenes other than v-Src (23). Caveolin expression was monitored in normal NIH 3T3 cells and compared with NIH 3T3 cells transformed with known oncogenes, such as bcr-abl, v-abl, middle T antigen, and activated Ras. In all cases, quantitation of caveolin protein expression revealed that the caveolin levels were dramatically reduced, from 25- to 100-fold depending on the specific oncogene examined. Transformed cells that expressed little or no caveolin did not contain any caveolae, as visualized by transmission electron microscopy (23). In addition, caveolin expression levels correlated inversely with the ability of these cells to grow in soft agar. That is, the cells expressing the least amount of caveolin and containing no detectable caveolae formed the largest colonies in soft agar. These results identify caveolin as a candidate tumor suppressor gene (23).

Recently, we have expressed caveolin in oncogenically transformed cells under the control of an inducible expression system (19). Regulated induction of caveolin expression was monitored by Western blot analysis and immunofluorescence microscopy. Our results indicate that the caveolin protein is

* This work was supported by a National Institutes of Health FIRST Award (to M. P. L.), a grant from the Elsa U. Pardee Foundation (to M. P. L.), a grant from the G. Harold and Leila Y. Mathers Charitable Foundation (to M. P. L. and P. E. S.), and a Scholarship in the Medical Sciences from the Charles E. Culpeper Foundation (to M. P. L.). The costs of publication of this article were defrayed in part by the payment of page charges. This article must therefore be hereby marked "*advertisement*" in accordance with 18 U.S.C. Section 1734 solely to indicate this fact.

¶ Contributed equally to this work.

§§ To whom correspondence should be addressed: 1300 Morris Park Ave., Bronx, NY 10461. Tel: 718-430-8828; Fax: 718-430-8830; E-mail: lisanti@aecom.yu.edu.

expressed well using this system and correctly localizes to the plasma membrane. Induction of caveolin expression in v-Abl-transformed and H-Ras (G12V)-transformed NIH 3T3 cells abrogated the anchorage-independent growth of these cells in soft agar, and resulted in the *de novo* formation of caveolae as seen by transmission electron microscopy (19). Consistent with its antagonism of Ras-mediated cell transformation, caveolin expression dramatically inhibited both Ras/mitogen-activated protein kinase-mediated and basal transcriptional activation of a mitogen-sensitive promoter (19). Using an established system to detect apoptotic cell death, it appears that the effects of caveolin may, in part, be attributed to its ability to initiate apoptosis in rapidly dividing cells (19). In addition, we find that caveolin expression levels are reversibly down-regulated by two distinct oncogenic stimuli. Taken together, our results indicate that down-regulation of caveolin expression and caveolae organelles may be critical to maintaining the transformed phenotype in certain cell populations (19).

Caveolin also interacts directly with signaling molecules, preferring their inactive conformation. Using a variety of domain-mapping approaches (deletion mutagenesis, glutathione *S*-transferase fusion proteins, and synthetic peptides), a region within caveolin has been defined that mediates the interaction of caveolin with itself and other proteins. This cytoplasmic 41-amino acid membrane proximal region of caveolin is sufficient to mediate the formation of caveolin homo-oligomers (14), and the C-terminal half of this region (20 amino acids; residues 82–101) mediates the interaction of caveolin with G-protein α subunits, H-Ras, and Src-family tyrosine kinases (24–26). This caveolin region preferentially recognizes the *inactive* conformation of these molecules, as mutationally activated G_α subunits (G_s; Q227L), v-Src, and H-Ras (G12V) fail to interact with caveolin (24–26). As this caveolin domain (residues 82–101) is critical for caveolin homo-oligomerization and the interaction of caveolin with certain caveolae-associated proteins (G-proteins, H-Ras, and Src-family kinases), we have previously termed this protein domain the *caveolin-scaffolding domain* or CSD (25, 27).

We have suggested that the caveolin scaffolding domain may function like other modular protein domains (SH-2, SH-3, PH, WW, and others) to generate membrane-bound oligomeric complexes that contain signaling molecules and cytoskeletal elements (2, 27). In essence, caveolin may act as molecular "velcro" to nucleate the formation of signal transduction complexes, holding these molecules in the off state. These findings would also explain the ability of caveolin expression to abrogate the anchorage-independent growth of cancerous/transformed cells (19).

Recent studies have shown that caveolin is only the first member of a growing gene family of caveolin proteins; caveolin has been re-termed caveolin-1. Three different caveolin genes (Cav-1, Cav-2, and Cav-3) encoding four different subtypes of caveolin have been described thus far (2). There are two subtypes of caveolin-1 (Cav-1α and Cav-1β) that differ in their respective translation initiation sites (28). The tissue distribution of caveolin-2 mRNA is extremely similar to caveolin-1 mRNA (5). In striking contrast, caveolin-3 mRNA and protein are expressed mainly in muscle tissue types (skeletal, cardiac, and smooth) (29–31).

Although caveolins-1 and -3 are now well-characterized, the study of caveolin-2 has been hampered by a lack of caveolin-2-specific antibody probes. Here, we have generated and characterized a novel mAb[1] probe that recognizes the caveolin-2 protein but not other known members of the caveolin gene family. Using this novel mAb probe, we (i) characterize the cell-type and tissue-specific expression of the caveolin-2 protein, (ii) report is co-expression, co-localization, and co-immunoprecipitation with caveolin-1, a well established caveolar marker protein, and (iii) demonstrate that caveolin-2 is localized to caveolae membranes as seen by immunoelectron microscopy.

EXPERIMENTAL PROCEDURES

Materials—The cDNAs for caveolins-1, -2, and -3 were as we described previously (5, 30, 32). Antibodies and their sources were as follows: anti-caveolin-1 IgG (mAb 2297; gift of Dr. John R. Glenney, Jr., Transduction Labs); anti-caveolin-1 IgG (mAb 2234; gift of Dr. John R. Glenney, Jr.); anti-myc epitope IgG (mAb 9E10; Santa Cruz Biotech); anti-caveolin-1 (pAb; rabbit anti-peptide antibody directed against caveolin-1 residues 2–21; Santa Cruz Biotech). A mAb directed against caveolin-3 (clone 26) was as we described previously (29). The anti-GDP dissociation inhibitor (GDI) antibody was a gift from Dr. Perry Bickel, Whitehead Institute, Cambridge, MA (33). A variety of other reagents were purchased commercially: fetal bovine serum (JRH Biosciences); pre-stained protein markers (Life Technologies, Inc.); Slow-Fade anti-fade reagent (Molecular Probes, Eugene, OR).

Hybridoma Production—A monoclonal antibody to caveolin-2 was generated by multiple immunizations of Balb/c female mice with a fusion protein encoding the full-length human caveolin-2 protein. Mice showing the highest titer of anti-caveolin-2 immunoreactivity were used to create fusions with myeloma cells using standard protocols (34). Positive hybridomas were cloned twice by limiting dilution and injected into mice to produce ascites fluid. IgGs were purified by affinity chromatography on protein A-Sepharose. These antibodies were produced in collaboration with Drs. Roberto Campos-Gonzalez and John R. Glenney, Jr. (Transduction Laboratories, Lexington, KY).

Transient Expression of Caveolin cDNAs in 293T Cells— Constructs encoding C-terminally myc-epitope-tagged forms of caveolin-1, -2, or -3 were as described previously (5, 28, 30). These constructs (~5–10 μg) were transiently transfected into 293T cells using standard calcium-phosphate precipitation. Forty-eight hours post-transfection, cells were scraped into lysis buffer (20 mM Tris, pH 8.0, 150 mM NaCl, 1% Triton X-100, 60 mM octyl-glucoside). Recombinant expression was analyzed by SDS-PAGE (15% acrylamide) followed by Western blotting. Epitope-tagged forms of caveolins-1, -2, and -3 were detected using the monoclonal antibody, 9E10, which recognizes the myc-epitope (EQKLISEEDLN).

Tissue Western—Approximately 200 mg of various mouse tissues were lysed in immunoprecipitation buffer and homogenized on ice with a Polytron tissue grinder, as described (4). Equal amounts (100 μg) were loaded on an SDS-PAGE gel (12% acrylamide). After transfer to nitrocellulose, the blot was probed with antibodies directed against caveolins-1, -2, -3 and GDI.

Immunofluorescence Microscopy—All reactions were performed at room temperature. 3T3-L1 fibroblasts were briefly washed three times with PBS and fixed for 45 min in PBS containing 3% paraformaldehyde. Fixed cells were rinsed with PBS and treated with 25 mM NH_4Cl in PBS for 10 min to quench free aldehyde groups. Cells were then permeabilized with 0.1% Triton X-100 for 10 min at room temperature and washed with PBS, four times at 10 min each. The cells were then successively incubated with PBS, 2% BSA containing: (i) a 1:200 dilution of anti-caveolin-2 IgG (mAb 65) and anti-caveolin-1 IgG (pAb; directed against caveolin-1 residues 2–21), and (ii) lissamine rhodamine B sulfonyl chloride-conjugated goat anti-mouse antibody (5 μg/ml) and fluorescein isothiocyanate-conjugated donkey anti-rabbit antibody (5 μg/ml). The first incubation was 30 min while primary and secondary antibody reactions were 60 min each. Cells were washed three times with PBS between incubations. Slides were mounted with Slow-Fade anti-fade reagent and observed under a Bio-Rad MR600 confocal fluorescence microscope.

Cell Culture Models of Adipocyte and Skeletal Muscle Differentiation—3T3-L1 mouse fibroblasts were propagated in 10-cm dishes and differentiated according to the conventional protocol (35). C2C12–3 cells (36) were derived from a single colony of C2C12 cells (37) cultured at clonal density and display a more stable phenotype than the parental cell line. C2C12–3 myoblasts were cultured as described elsewhere (36). Briefly, proliferating C2C12–3 cells were cultured in high mitogen

[1] The abbreviations used are: mAb, monoclonal antibody; pAb, polyclonal antibody; GDI, GDP dissociation inhibitor; PAGE, polyacrylamide gel electrophoresis; PBS, phosphate-buffered saline; CHO, Chinese hamster ovary; IPTG, isopropyl-1-thio-β-D-galactopyranoside; Mes, 4-morpholineethanesulfonic acid.

medium (Dulbecco's modified Eagle's containing 15% fetal bovine serum and 1% chicken embryo extract) and induced to differentiate at confluence in low mitogen medium (Dulbecco's modified Eagle's containing 3% horse serum). Overt differentiation was indicated by the assembly of multi-nucleated syncytia, which commenced 36–48 h after the cells were switched to low mitogen media.

Velocity Gradient Centrifugation—Estimation of the molecular mass of caveolin-2 was performed as described previously for caveolin-1 (14). Briefly, samples were dissociated by incubation with 500 μl of Mes-buffered saline (25 mM, pH 6.5, 0.15 M NaCl) plus 60 mM octyl-glucoside. Solubilized material was then loaded atop a 5–40% linear sucrose gradient (4.3 ml) and centrifuged at 50,000 rpm (~340,000 × *g*) for 10 h in a SW-60 rotor (Beckman Instruments, Palo Alto, CA). Note that the entire gradient was prepared in MBS plus 60 mM octyl-glucoside. After centrifugation, gradient fractions were collected from the top. Molecular mass standards for velocity gradient centrifugation were as follows: carbonic anhydrase (29 kDa); bovine serum albumin (66 kDa); alcohol dehydrogenase (150 kDa); β-amylase (200 kDa); apoferritin (443 kDa) (Sigma).

Immunoblotting—Samples were separated by SDS-PAGE (15% acrylamide) and transferred to nitrocellulose. After transfer, nitrocellulose sheets were stained with Ponceau S to visualize protein bands and subjected to immunoblotting. For immunoblotting, incubation conditions were as described by the manufacturer (Amersham Life Science, Inc.), except that we supplemented our blocking solution with both 1% bovine serum albumin and 1% non-fat dry milk (Carnation).

Immunoprecipitation—Immunoprecipitations were carried out using protein-A Sepharose CL-4B (Pharmacia Biotech Inc.) as described previously (38), with minor modifications. Briefly, cells were lysed in a buffer containing 10 mM Tris, pH 8.0, 0.15 M NaCl, 5 mM EDTA, 1% Triton X-100, 60 mM octyl-glucoside and subjected to immunoprecipitation with anti-caveolin-1 (mAb 2234) or anti-caveolin-2 (mAb 65). After extensive washing, samples were separated by SDS-PAGE (15% acrylamide) and transferred to nitrocellulose. Blots were then probed with IgGs directed against caveolin-1 (mAb 2297) or caveolin-2 (mAb 65).

Immunogold Electron Microscopy—The procedures used were as described previously (39). Briefly, samples were fixed in 2% paraformaldehyde in 0.1 M phosphate buffer at pH 7.4 for 24 h at room temperature. Cells were transferred in 0.2% paraformaldehyde, scraped, and collected. Samples were then processed for cryo-electron microscopy using a Leica ultra-cryomicrotome and Diatome diamond knife. Sections of 45 nm were cut at −125 °C and collected with a mixture of sucrose and cellulose (40). Cryosections were incubated at room temperature with antibodies for 30 min, washed, and incubated for 20 min with protein A gold. Electron micrographs were made with a JEOL 1010 electron microscope at 80 kV.

Immunostaining of Human Skeletal Muscle Tissue—All solutions were prepared in PBS. Frozen sections (4–6 μm) from normal human muscle biopsies were fixed with 4% paraformaldehyde and blocked for 1 h with 5% horse serum and 5% non-fat dry milk. Primary antibodies were diluted in blocking solution (1:400) and incubated at 4 °C overnight. After washing 4 times, sections were incubated with horseradish peroxidase-conjugated anti-mouse antibody (diluted 1:1,500) for 2 h at 4 °C. To visualized bound secondary antibodies, sections were further incubated with 3,3′-diaminobenzidine (1 mg/ml) and 0.03% hydrogen peroxide. Note that endogenous peroxidase activities were inactivated after fixation and prior to antibody incubations.

RESULTS

Generation and Characterization of a mAb Probe Specific for Caveolin-2—Caveolins-1, -2, and -3 are distinct gene products with different molecular masses, all in the range of ~18–24 kDa (5, 28, 30, 31). Currently, there are no available antibody probes that selectively recognize caveolin-2. Thus, a fusion protein carrying the full-length human caveolin-2 protein was used to generate a caveolin-2 specific monoclonal antibody probe. Fig. 1 (*bottom panel*) demonstrates the specificity of this novel mAb probe; it selectively recognizes caveolin-2, but does not recognize caveolin-1 or -3.

Thus, this novel mAb probe can be used, in conjunction with other published antibodies directed against caveolins-1 and -3 (28, 29, 41), to study the function and differential expression of distinct caveolin gene family members.

Cell-type and Tissue-specific Expression of the Caveolin-2 Protein—To identify model cell systems to study caveolin-2, we

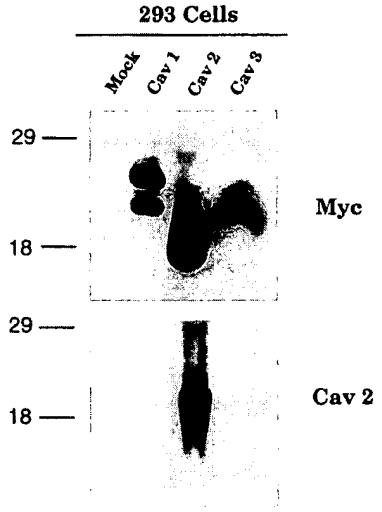

FIG. 1. **Characterization of a mAb probe specific for caveolin-2.** Caveolins-1, -2, and -3 are distinct gene products with different molecular masses, all in the range of ~18–24 kDa. C-terminal myc-tagged forms of caveolins-1, -2, and -3 were transiently expressed in 293T cells. Lysates were generated and used to determine the specificity of caveolin antibody probes by immunoblotting. As a control for equal loading, immunoblotting was first performed with mAb 9E10 that recognizes the myc-epitope; this antibody reveals all three myc-tagged caveolin gene products (*top panel*). Note that mAb 65 only recognizes caveolin-2 (*bottom panel*). Molecular weight markers are as indicated.

examined the expression of caveolin-2 in a variety of commonly used cell lines and primary cultured cells (Fig. 2). The expression patterns of caveolins-1 and -3 are shown for comparison; antibodies to the ubiquitously expressed GDI were used to confirm equal loading. Note that caveolin-2 is most widely expressed, whereas caveolin-1 shows a more restricted distribution, and caveolin-3 is found only within a cell line derived from skeletal muscle. More specifically, caveolin-2 is most abundant in endothelial cells, smooth muscle cells, skeletal myoblasts (L6 and BC3H1), fibroblasts, and 3T3-L1 adipocytes. Thus, the expression of caveolin-2 protein most closely parallels the distribution of caveolin-1. Also, it is important to note that L6 myoblasts are the only cell line that expresses all three caveolins simultaneously.

To establish the tissue distribution of caveolin-2 protein, we prepared extracts from a number of different murine tissues (Fig. 3*A*). The tissue distribution of caveolins-1 and-3 are shown for comparison; again, to ensure equal protein loading in all lanes, we also probed these blots with anti-GDI antibodies. Caveolin-2 is detected mainly in adipose and lung tissues, although longer exposures demonstrate a lower level of caveolin-2 expression in most tissue types. This is consistent with (i) our previous work demonstrating that caveolin-2 mRNA is most abundant in white adipose tissue, differentiated 3T3-L1 adipocytes, and lung tissue (5) and (ii) with previous morphological evidence suggesting that differentiated 3T3-L1 adipocytes are a rich source of caveolae (3, 4).

Caveolin-2 Protein Is Induced during Adipocyte Differentiation—Cultured 3T3-L1 fibroblasts offer a convenient system to study adipocyte differentiation (3). These cells can be induced to differentiate over a period of 8 days from precursor fibroblasts into adipocytes. Caveolin-2 protein is strongly induced between 2 and 10 days of differentiation (Fig. 3*B*, *top panel*). Note that the expression of caveolin-2 is induced ~10–20-fold. The expression of an adipocyte-specific secretory protein (Acrp30; Ref. 42) is included as a positive control for the differentiation process (Fig. 3*B*, *bottom panel*).

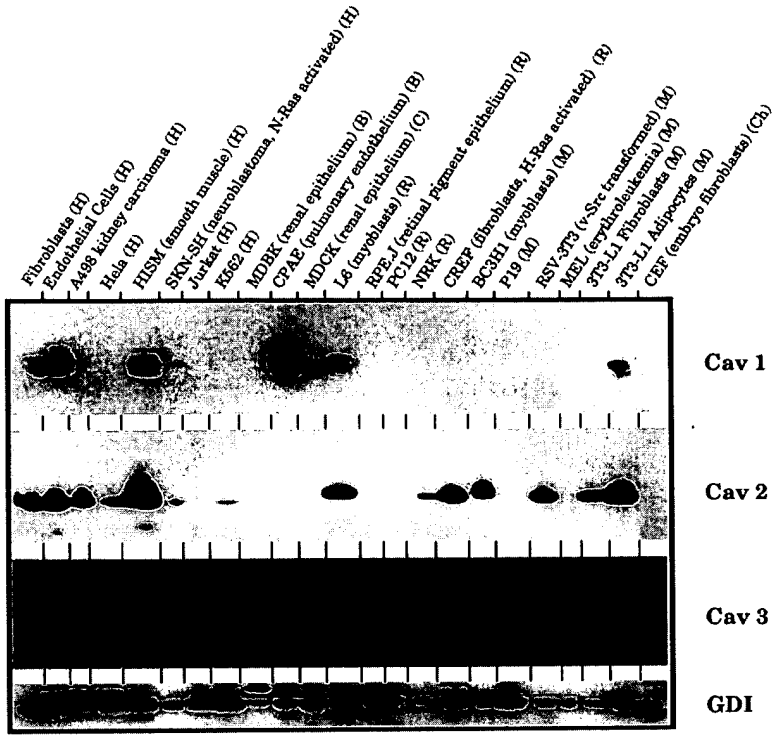

FIG. 2. **Expression of caveolin-2 in established cell lines and primary cultured cells.** 10 μg of total cellular protein extracted from a given cell line (as indicated) was separated by SDS-PAGE (13% acrylamide gel), transferred to nitrocellulose, and probed with anti-caveolin-1 IgG (mAb 2297; *first panel*), anti-caveolin-2 IgG (mAb 65; *second panel*), anti-caveolin-3 IgG (mAb 26; *third panel*), and anti-GDI IgG (rabbit polyclonal; *fourth panel*). *R*, rat; *H*, human; *B*, bovine; *C*, canine; *M*, murine; and *Ch*, chicken.

Caveolins-1 and -2 Form a Stable Hetero-oligomeric Complex—Given the similarity between the tissue and cellular distributions of caveolins 1 and 2, we wondered whether these two distinct caveolin gene products interact *in vivo*. To address this issue, we performed a series of co-immunoprecipitation experiments. 3T3-L1 adipocytes were lysed and subjected to immunoprecipitation with a mAb directed against caveolin-1 (2234) that recognizes a unique N-terminal epitope that is not found in other caveolin family members (28). These immunoprecipitates were then probed by Western analysis using anti-caveolin-2 IgG (mAb 65). Conversely, lysates were also immunoprecipitated with IgGs directed against caveolin-2 and then probed by Western analysis using anti-caveolin-1 IgG (mAb 2297).

Fig. 4 demonstrates that mAb 2234 directed against caveolin-1 (28) can be used to co-immunoprecipitate both caveolins-1 and -2. In addition, mAb 65 directed against caveolin-2 can be used to co-immunoprecipitate both caveolins-1 and -2. This is despite the fact that these antibodies are monospecific as determined by Western blot analysis (Ref. 28, and this report). Thus, it appears that caveolins 1 and 2 form a stable complex *in vivo*.

To estimate the amount of caveolin-2 that forms a complex with caveolin-1, a 3T3-L1 adipocyte lysate was divided into two parts. Part A was loaded directly onto an SDS-PAGE gel to quantitate the total amount of caveolin-2 in the extract. Part B was immunoprecipitated with anti-caveolin-1 IgG (mAb 2234). Fig. 5 shows that immunoprecipitation of the lysate with anti-caveolin-1 IgG (mAb 2234) resulted in a dramatic reduction of the caveolin-2 signal by >90%. These results clearly demonstrate that under steady-state conditions the bulk of caveolin-2 is associated with caveolin-1.

Immunolocalization of Caveolin-2 to the Plasma Membrane and Intracellular Membranes: Co-localization with Caveolin-1—To further examine whether caveolins 1 and 2 are physically associated as a discrete complex in intact cells, we performed double-labeling with mAb 65 (caveolin-2-specific) and an anti-caveolin-1-specific polyclonal IgG directed against a unique N-terminal region of caveolin-1 (residues 2–21). These two primary antibodies were chosen for double-labeling experiments as they were elicited in different animal species (mouse *versus* rabbit), minimizing possible cross-reaction of the individual primary antibodies with distinctly tagged secondary antibodies. Immunostaining was visualized by traditional fluorescence microscopy.

The immunostaining pattern obtained in 3T3-L1 fibroblasts with caveolin-2 is very similar to immunostaining patterns observed previously for caveolins-1 and -3 (data not shown) (5, 12, 13, 28, 30–32). Many small micro-patches are present throughout the cell and along the cell surface. In addition, double-labeling experiments employing 3T3-L1 fibroblasts that co-express caveolin-1 and caveolin-2 demonstrate significant co-localization of these two distinct gene products (not shown). The intense immunostaining may represent the leading edge of the cell as caveolae are known to be morphologically concentrated in this area of the cell (12).

As our initial experiments using traditional fluorescence microscopy showed co-localization of caveolins 1 and 2, we used confocal laser scanning microscopy to more stringently assess their co-localization. Fig. 6*A* shows a series of optical sections taken from the top (*panel 1*) to the bottom (*panel 10*) of a single 3T3-L1 fibroblast. A stacked composite of these images is presented in Fig. 6*B*. Note that in all the optical planes examined, caveolins-1 and -2 demonstrate the same pattern of localization, indicating that these two caveolins co-exist within the same regions of a given cell.

Ultrastructural Localization of Caveolin-2 to Caveolae Membranes by Immunoelectron Microscopy—Using ultrathin cryosections, we next explored the ultrastructural localization of caveolin-2 by immunoelectron microscopy. Fig. 7 shows the distribution of caveolin-2 in a fibroblastic cell line (CHO cells, *panel A*) and endothelial cells (*panel B*) derived from a human skin biopsy. In CHO cells, immunogold labeling is specifically associated with caveolae (see *arrows*). In endothelial cells, caveolae on both luminal and basolateral sides of the cell were stained by immunogold labeling with anti-caveolin-2 IgG (mAb 65). In contrast, mitochondria, endoplasmic reticulum, the nu-

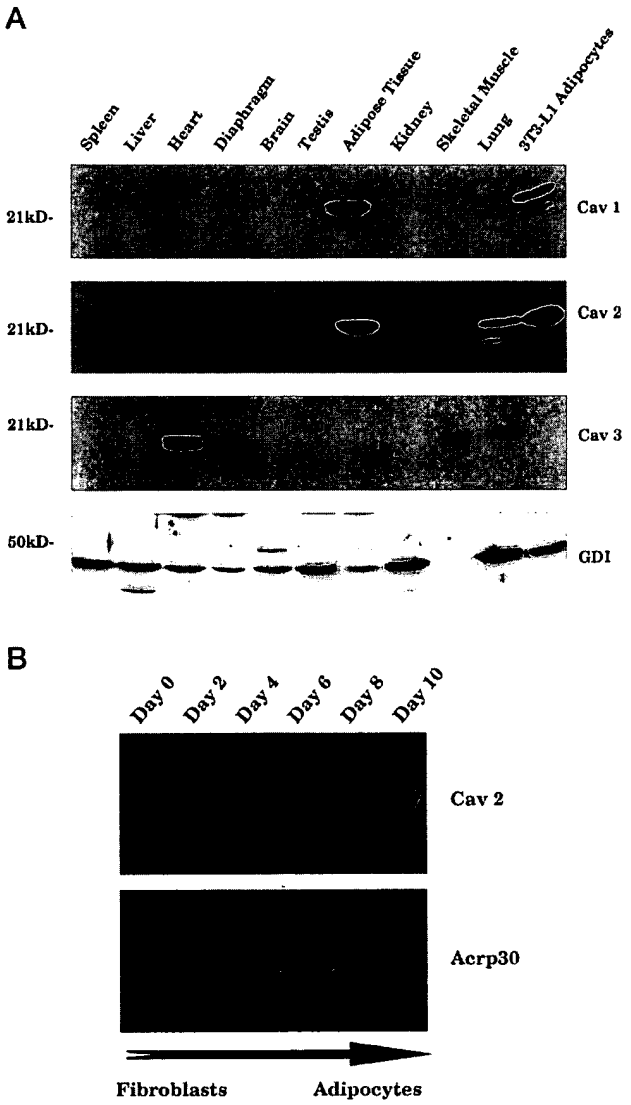

FIG. 3. **Western blot analysis of the tissue distribution of caveolin-2: induction of caveolin-2 protein during adipocyte differentiation.** *A*, tissue Western. Extracts of mouse tissues were prepared as described under "Experimental Procedures". In addition, a lane containing differentiated 3T3-L1 adipocytes was included as a comparison. After SDS-PAGE and transfer to nitrocellulose, blots were probed with anti-caveolin IgG. *First panel*, caveolin-1 (mAb 2297); *second panel*, caveolin-2 (mAb 65); *third panel*, caveolin-3 (mAb 26); and *fourth panel*, GDI polyclonal IgG (as a control for equal loading). Caveolins-1 and -2 are most abundantly expressed in adipose tissue and 3T3-L1 adipocytes. Note that the lane containing skeletal muscle is underloaded as judged by the low signal obtained for GDI immunoblotting. *B*, adipocyte differentiation. 50 μg of total cellular protein extracted from 3T3-L1 fibroblasts and 3T3-L1 adipocytes (days 2, 4, 6, 8, and 10) were separated by SDS-PAGE, transferred to nitrocellulose, and probed with anti-caveolin-2 (mAb 65; *top panel*) or anti-Acrp30 (rabbit polyclonal IgG; *bottom panel*). Note that caveolin-2 and Acrp30 (an adipocyte-specific secretory protein) are both dramatically induced during adipocyte differentiation. Acrp30 served as a positive control for differentiation.

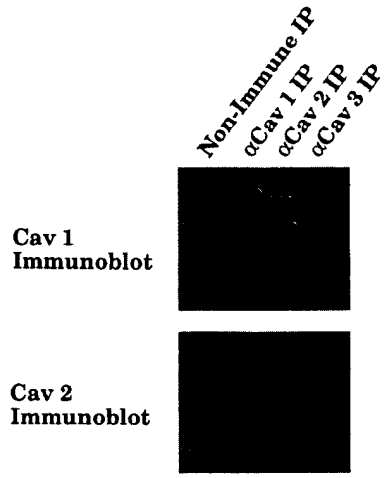

FIG. 4. **Caveolins 1 and 2 form a stable hetero-oligomeric complex.** 3T3-L1 fibroblasts were lysed and subjected to immunoprecipitation with anti-caveolin-1 IgG (mAb 2234) that recognizes a unique N-terminal epitope that is not found in other caveolin family members (28). These immunoprecipitates were then probed by Western analysis using anti-caveolin-2 IgG (mAb 65). Conversely, lysates were also immunoprecipitated with IgGs directed against caveolin-2 (mAb 65) and then probed by Western analysis using anti-caveolin-1 IgG (mAb 2297). Immunoprecipitation with anti-caveolin-3 IgG (mAb 26) was included as a negative control as the expression of caveolin-3 is muscle specific. Note that anti-caveolin-1 IgG (mAb 2234) can be used to co-immunoprecipitate both caveolins-1 and -2. In addition, mAb 65 directed against caveolin-2 can be used to co-immunoprecipitate both caveolins-1 and -2. Thus, it appears that caveolins 1 and 2 form a stable complex *in vivo*.

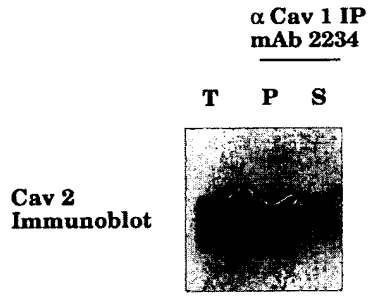

FIG. 5. **A significant fraction of total caveolin-2 is associated with caveolin-1 at steady-state.** One 10-cm plate of 3T3-L1 adipocytes was lysed as described under "Experimental Procedures." Prior to the immunoprecipitation, 5% of the total lysate was removed (*T*, Total). The remaining 95% was subsequently immunoprecipitated with anti-caveolin-1 IgG (mAb 2234); 5% of the resulting immunoprecipitate (*P*, Pellet) and 5% of the remaining supernatant after the extract was immunodepleted for caveolin 1 (*S*, Supernatant) were then analyzed by SDS-PAGE/Western blotting and probed with anti-caveolin-2 IgG. Note that >90% of caveolin-2 was recovered with anti-caveolin-1 IgG (mAb 2234).

cleus, endosomes, intermediate filaments, the basal lamina, and erythrocytes remained completely unlabeled by this technique. Immunogold labeling of caveolae within endothelial cells is consistent with our observation that caveolin-2 is abundantly expressed in endothelial cells by Western blot analysis (Fig. 2).

Differential Expression of Caveolins-1 and -2 in Oncogenically Transformed NIH 3T3 Cells—Modification and/or inactivation of caveolin-1 expression appears to be a common feature of the transformed phenotype. Historically, caveolin-1 was first identified as a major v-Src substrate in Rous sarcoma virus-transformed cells (9). Based on this observation, it has been proposed that caveolin-1 may represent a critical target during cell transformation (9, 10). In direct support of this notion, caveolin-1 mRNA and protein expression are reduced or absent in NIH 3T3 cells transformed by a variety of activated oncogenes (such as v-Abl and H-Ras (G12V)); caveolae organelles are also missing from these transformed cells (23). However, it remains unknown whether caveolin-2 is down-regulated in response to oncogenic transformation.

Fig. 8*A* shows that while caveolin-1 expression is dramatically down-regulated in v-Abl and H-Ras (G12V)-transformed

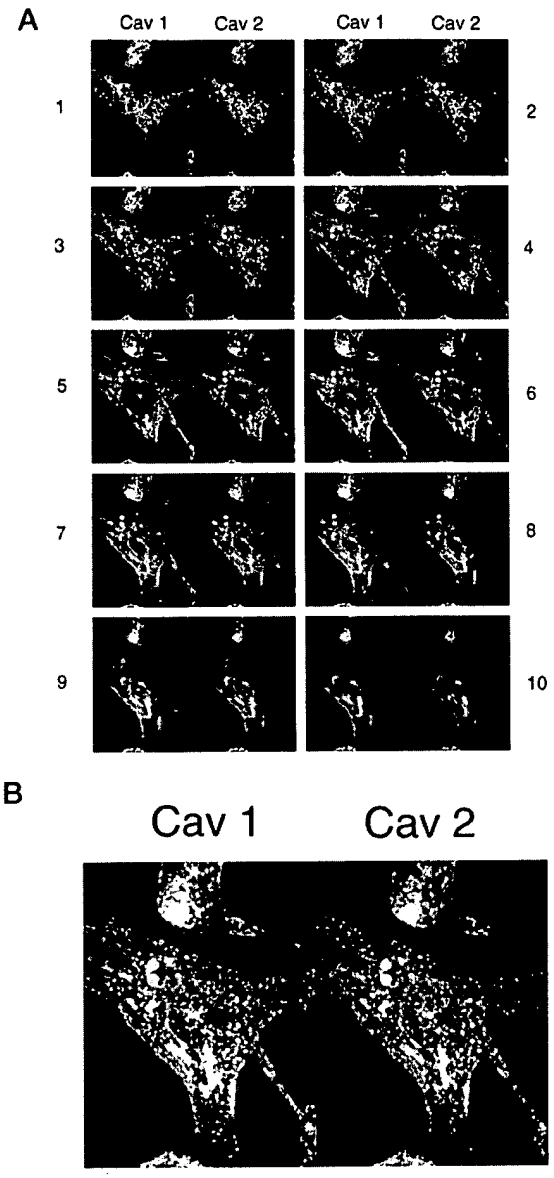

FIG. 6. **Immunolocalization of caveolin-2 in 3T3-L1 fibroblasts by laser scanning confocal microscopy.** *A*, cells were doubly immunostained with a mouse mAb directed against caveolin-2 (mAb 65) and a rabbit polyclonal antibody directed against the unique N terminus of caveolin-1 (residues 2–21). Bound primary antibodies were visualized by incubation with distinctly tagged fluorescent secondary antibodies; see "Experimental Procedures." Note that caveolins-1 and -2 are co-localized to the same areas of the plasma membrane and internal membranes. A series of ten optical sections from the top (*panel 1*) to the bottom (*panel 10*) of a single cell are shown. Each individual panel shows: *left*, caveolin-1 immunostaining (FITC, fluorescein isothiocyanate); *right*, caveolin-2 immunostaining (LRSC, lissamine rhodamine B sulfonyl chloride). Note the dramatic co-localization within each optical plane. *B*, a stacked summation of all ten sections is shown.

NIH 3T3 cells, caveolin-2 expression remains virtually unaffected in v-Abl transformed cells and is slightly induced (~2-fold) in H-Ras (G12V) transformed cells. As we have previously demonstrated that these transformed cells do not contain detectable caveolae (23), it appears that expression of caveolin-2 is not sufficient to drive caveolae formation. Thus, caveolin-2 can be expressed within cells that lack morphologically distinguishable caveolae.

As caveolin-1 forms a high molecular mass oligomeric complex (14, 15), we wondered if low levels of caveolin-1 expression would affect the oligomeric state of caveolin-2. Thus, we compared the size of caveolin-2 complexes in normal and v-Abl transformed NIH 3T3 cells (Fig. 8*B*). Our results indicate that in v-Abl transformed cells that lack normal levels of caveolin-1 expression, a significant fraction of caveolin-2 was present in the monomeric or dimeric state. This is consistent with our previous results demonstrating that recombinant over-expression of caveolin-2 in Cos-7 cells yields primarily dimeric and monomeric caveolin-2 (5). However, in normal NIH 3T3 cells that express caveolin-1, all of the caveolin-2 was present within large oligomeric complexes (>150 kDa). These results suggest that caveolin-1 co-expression facilitates the formation of high molecular mass complexes that contain both caveolins 1 and 2.

The distribution of recombinantly over-expressed caveolin-2 after transient expression in Cos-7 cells is shown for comparison; recombinant caveolin-2 was detected using mAb 9E10 that recognizes the myc-epitope (Fig. 8*B*). In contrast to endogenous caveolin-2, recombinantly over-expressed caveolin-2 behaves mainly as a dimer in these velocity gradients (5).

Caveolin-1 Embeds Caveolin-2 Tightly within a Hetero-oligomeric Complex—During the course of the current studies, we noticed that there are higher levels of caveolin-2 in immunoprecipitates generated with anti-caveolin-1 IgG than in immunoprecipitates generated with caveolin-2 IgG directly. Given that the anti-caveolin-1 mAb does not cross-react with caveolin-2, we found this observation quite surprising.

A possible explanation for this phenomenon is epitope masking, in which caveolin-1 binding to caveolin-2 would block access to the epitope recognized by the anti-caveolin-2 IgG. To test this hypothesis, we took advantage of a v-Abl-transformed cell line that harbors a copy of the caveolin-1 cDNA under the control of the lacZ promoter (19). While these cells express very low levels of endogenous caveolin-1 due to transformation, caveolin-1 expression levels can be dramatically induced in the presence of IPTG.

Fig. 9 shows that in the absence of IPTG, *i.e.* very low levels of caveolin-1, small amounts of caveolin-2 can be recovered with anti-caveolin-1 IgG (*first lane*). Upon induction of caveolin-1, increased levels of caveolin-2 can be recovered with anti-caveolin-1 IgG in agreement with increased incorporation of caveolin-2 into caveolin-1 containing complexes (*second lane*). However, induction of caveolin-1 decreases the amount of caveolin-2 signal that can be recovered with anti-caveolin-2 IgG (*third* and *fourth lanes*).

This observation is in line with our hypothesis that caveolin-1 binding to caveolin-2 masks the epitope recognized by the caveolin-2 IgG. In addition, control experiments confirmed that total caveolin-2 levels remained constant before and after induction of caveolin-1 (not shown). Hence, we conclude that caveolin-2 molecules are tightly embedded within the caveolin-1 oligomer.

Caveolin-2 Is Constitutively Expressed in C2C12 Myoblasts and Myotubes—Cultured C2C12 cells offer a convenient system to study skeletal myoblast differentiation. These cells can be induced to differentiate from myoblasts into myotubes bearing an embryonic phenotype in low mitogen medium over a period of 2 days (36, 37). We and others have previously shown that caveolin-3 mRNA and protein are undetectable in precursor myoblasts and are strongly induced during myoblast differentiation (29–31). In contrast, no caveolin-1 expression was detected in either precursor myoblasts or differentiated myotubes (29, 30). These results are consistent with the selective expression of caveolin-3 in skeletal muscle and other muscle tissues (29–31) and suggest that caveolin-3 may function in muscle from the earliest stages of its development.

As caveolin-2 was expressed in L6 and BC3H1 skeletal myo-

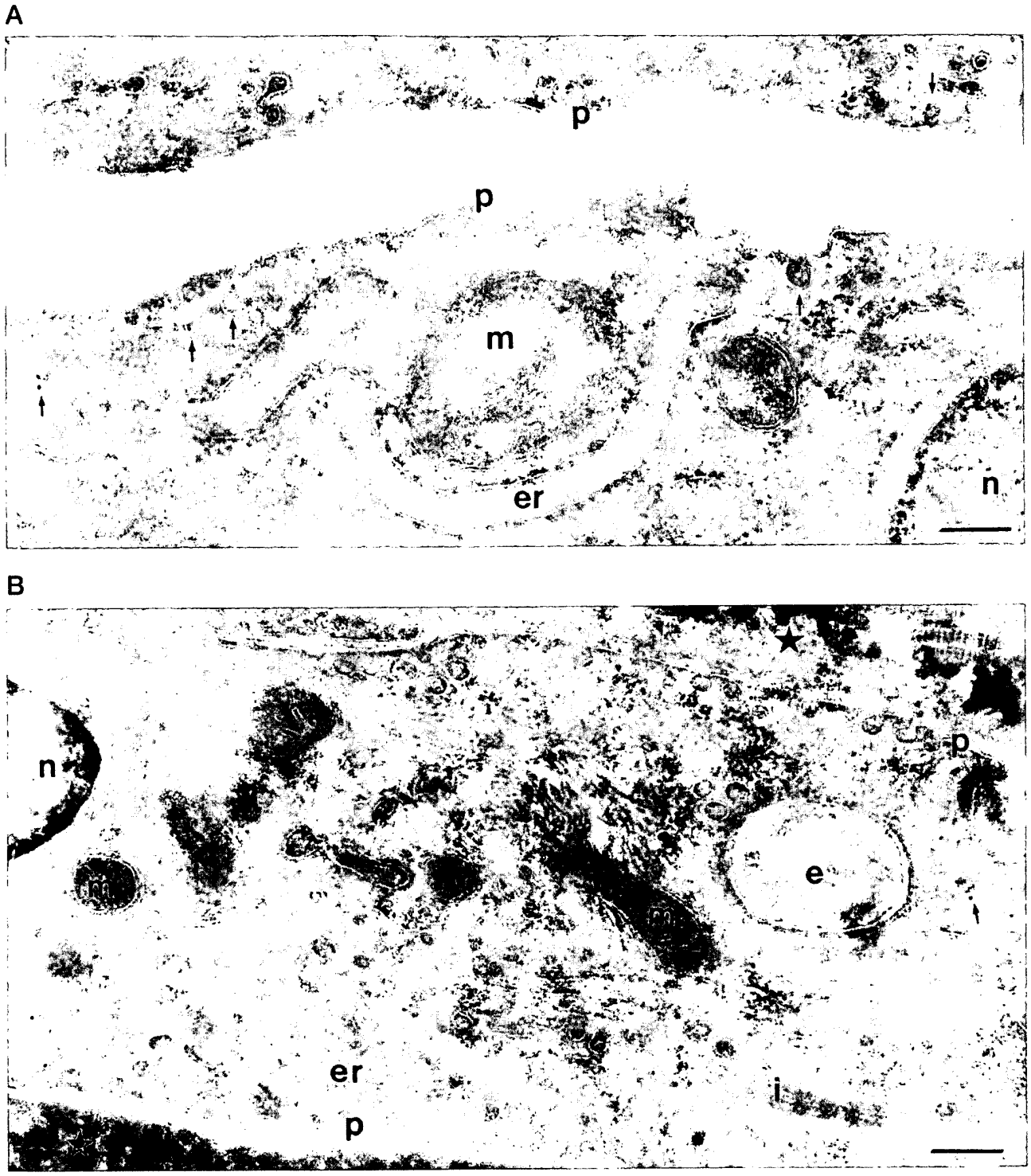

FIG. 7. **Immunoelectron microscopic localization of caveolin-2.** Ultrathin cryo-sections were labeled with anti-caveolin-2 IgG (mAb 65) as described under "Experimental Procedures." *A*, electron micrograph of a fibroblastic cell type (a CHO cell). Note that immunogold labeling is specifically associated with caveolae (see *arrows*). *B*, electron micrograph of an endothelial cell derived from a human skin biopsy. Note the immunogold labeling of caveolae on both luminal and basolateral sides of the endothelial cell. *Bars* = 200 nm. *p*, plasma membrane; *m*, mitochondria; *er*, endoplasmic reticulum; *n*, nucleus; *e*, endosome; *i*, intermediate filament; *closed star*, basal lamina, *open star*, erythrocyte.

blasts (Fig. 2), we assessed whether caveolin-2 is induced during differentiation of C2C12 cells from myoblasts to myotubes. Fig. 10 shows that caveolin-2 levels remained constant during this process of differentiation. As a positive control for the differentiation process, we also assessed the induction of caveolin-3 within the same samples. In contrast, caveolin-3 was dramatically induced during the transition from myoblasts to myotubes. These results suggest that the expression of caveolins 2 and 3 are independently regulated within skeletal muscle fibers.

Localization of Caveolin-2 within Bona Fide Skeletal Muscle Tissue—Given that caveolin-2 was constitutively expressed in

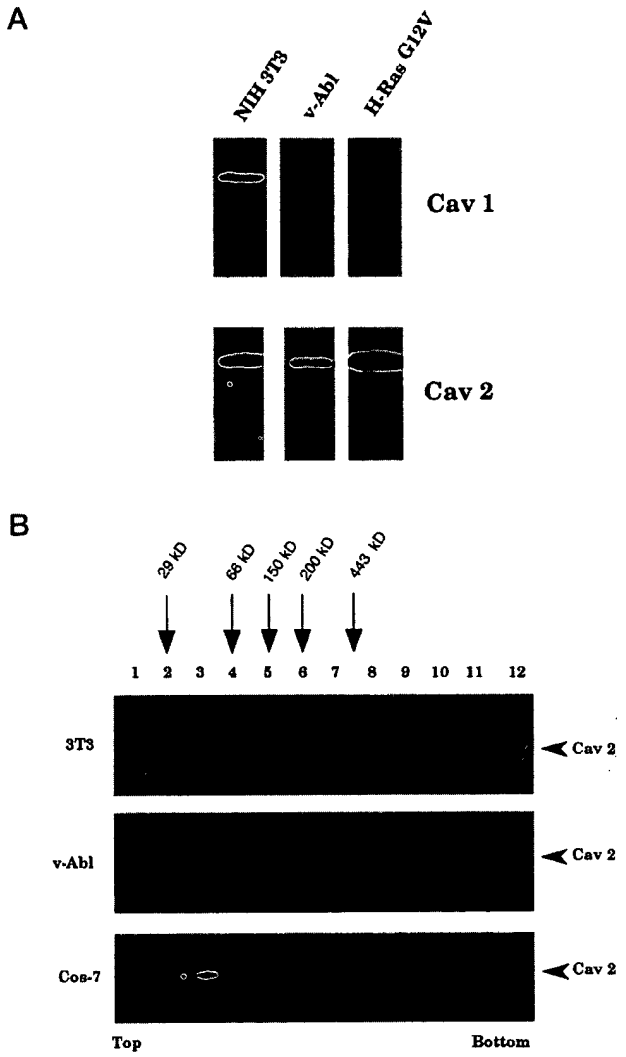

FIG. 8. **Expression of caveolin-2 in normal and transformed NIH 3T3 cells.** *A*, lysates were prepared from normal and transformed (v-Abl and H-Ras (G12V)) NIH 3T3 cells and subjected to immunoblot analysis with anti-caveolin-1 IgG (mAb 2297) or anti-caveolin-2 IgG (mAb 65). Note that caveolin-1 expression is dramatically down-regulated in v-Abl and H-Ras (G12V)-transformed NIH 3T3 cells, whereas caveolin-2 expression remains virtually unaffected in v-Abl transformed cells and is slightly induced (~2-fold) in H-Ras (G12V) transformed cells. Each lane contains ~50 μg of protein lysate. *B*, velocity gradient analysis of caveolin-2. Normal and v-Abl-transformed NIH 3T3 cells were solubilized, loaded atop a 5–40% sucrose density gradient and subjected to centrifugation for 10 h, as we described previously for caveolin-1 (14). The distribution of endogenous caveolin-2 was detected by immunoblot analysis with anti-caveolin-2 IgG (mAb 65). *Arrows* mark the positions of molecular mass standards. The distribution of recombinantly over-expressed caveolin-2 after transient expression in Cos-7 cells is shown for comparison; recombinant caveolin-2 was detected using mAb 9E10 that recognizes the myc-epitope. In contrast to endogenous caveolin-2, recombinantly over-expressed caveolin-2 behaves as a dimer in these velocity gradients as we have shown previously (5).

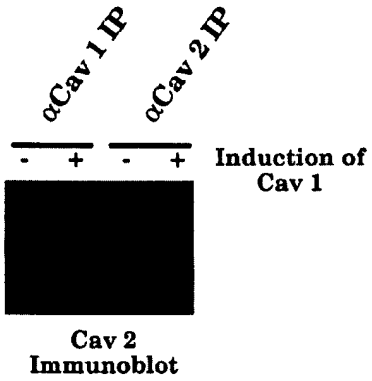

FIG. 9. **Induction of caveolin-1 protein expression promotes complex formation between caveolins 1 and 2.** v-Abl transformed NIH-3T3 cells were transfected with caveolin-1 under the control of an IPTG-inducible promoter (19). In this cell line, addition of 5 mM IPTG for 24 h dramatically induces the expression of caveolin-1, as we have recently described (19). v-Abl cells were lysed before or after induction of caveolin-1 expression and subjected to immunoprecipitation with IgG directed against either caveolin-1 (mAb 2234) or caveolin-2 (mAb 65). After SDS-PAGE and transfer to nitrocellulose, these immunoprecipitates were analyzed by Western blotting to detect the presence of caveolin-2 within these complexes. Note that induction of caveolin-1 expression (i) enhances the ability of anti-caveolin-1 IgG to co-immunoprecipitate caveolin-2; and (ii) inhibits the ability of anti-caveolin-2 IgG to immunoprecipitate caveolin-2. These results suggest that complex formation between caveolins-1 and -2 can mask the antibody epitope that is recognized by anti-caveolin-2 IgG (mAb 65).

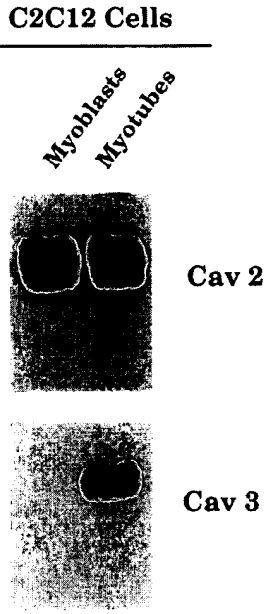

FIG. 10. **Differential expression of caveolins-2 and -3 in C2C12 myoblasts and myotubes.** Cell lysates were prepared from C2C12 myoblasts and myotubes and subjected to immunoblot analysis with anti-caveolin-2 IgG (mAb 65) (*top panel*) or anti-caveolin-3 IgG (mAb 26) (*bottom panel*). Note that caveolin-3 expression is selectively induced during myoblast differentiation while the expression of caveolin-2 remains unchanged. No expression of caveolin-1 was detected using the same cell extracts (not shown).

three distinct myoblast cell lines (L6, BC3H1, and C2C12) and within differentiated C2C12 myotubes, we next examined the localization of caveolin-2 within human skeletal muscle tissue. Fig. 11 shows that caveolin-2 is primarily expressed within the endothelial cells that line the blood vessels that run between the muscle fibers but not within the myofibers themselves. The distribution of caveolin-3 is shown for comparison. Note that caveolin-3 immunostaining is confined to the sarcolemma (plasma membrane) of the myofibers and is not detected within any other cell types. Thus, co-expression of caveolins-2 and -3 in myoblasts and myotubes does not reflect the state of their expression within human adult skeletal muscle tissue.

DISCUSSION

Caveolins-1, -2, and -3 are a family of cytoplasmic membrane-anchored scaffolding proteins that (i) help to sculpt caveolae membranes from the plasma membrane proper and

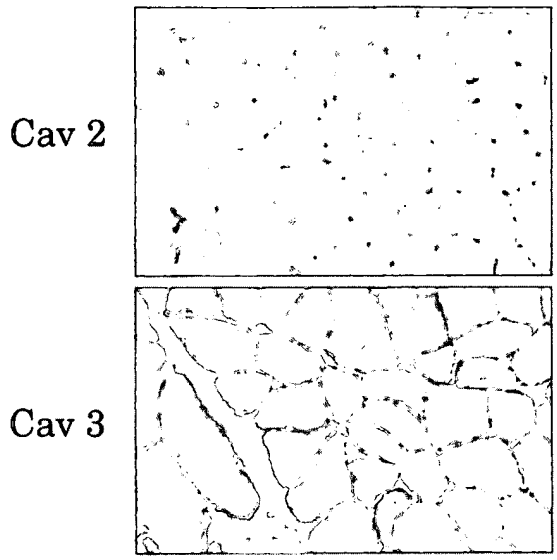

FIG. 11. **Immunolocalization of caveolins 2 and 3 within bona fide skeletal muscle tissue.** Two consecutive parallel sections derived from a human skeletal muscle biopsy were immunostained with either anti-caveolin-2 IgG (mAb 65; *top panel*) or anti-caveolin-3 IgG (mAb 26; *bottom panel*). Bound primary antibodies were visualized with the appropriate horseradish peroxidase-conjugated secondary antibody. Note that caveolin-2 is primarily expressed within the endothelial cells that line the blood vessels, while caveolin-3 is localized to the sarcolemma (plasma membrane) of the myofibers.

(ii) participate in the sequestration of inactive signaling molecules (reviewed within Ref. 2). Although caveolins-1 and -3 are now well-characterized, the study of caveolin-2 has been hampered by a lack of caveolin-2-specific antibody probes. Only the distribution of caveolin-2 mRNA was previously studied, and a recombinant epitope-tagged form of the protein has been expressed in cultured cells (5).

Here, we have generated and characterized a novel mAb probe that recognizes the *native endogenous* caveolin-2 protein but not other known members of the caveolin gene family. This novel probe will greatly facilitate the study of caveolae in adipocytes, endothelial cells, and smooth and striated muscle cells as caveolin-2 is the most widely expressed caveolin family member observed to date. Caveolin-2 is highly expressed in many cell lines that fail to express caveolin-1, suggesting that caveolin-2 does not absolutely require caveolin-1 for its expression.

Immunolocalization of caveolin-2 in 3T3-L1 fibroblasts reveals that caveolin-2 is localized to the plasma membrane and internal membranes; this immunostaining pattern strictly coincides with the subcellular distribution of caveolin-1 within the same cell. In line with these observations, co-immunoprecipitation experiments clearly demonstrate that caveolins 1 and 2 form a stable hetero-oligomeric complex *in vivo*. This is consistent with our previous report demonstrating that the mRNA's for caveolins 1 and 2 are co-expressed within the same cell types and both mRNA species are co-induced during adipocyte differentiation (5).

We have previously described the existence of caveolin-1 homo-oligomeric complexes (14). This was at a time when we had no concrete evidence for the existence of additional caveolin genes. A host of experiments prompted us to conclude that caveolin-1 exists as a homo-oligomeric complex. These studies were performed mainly in MDCK cells. Interestingly, MDCK cells are peculiar in that they express caveolin-1 but very little if any caveolin-2 (See Fig. 2). As such, they are an exception since we find here that caveolins-1 and -2 are co-expressed in most other cell systems. However, this does explain our initial findings that caveolin-1 forms a homo-oligomeric complex in MDCK cells (14). In addition, we have shown that purified recombinant caveolin-1 expressed in *E. coli* and Sf 21 insect cells is sufficient to form caveolin-1 homo-oligomers of the same size as native endogenous caveolin-1 (14, 18, 21).

Perhaps surprisingly, we find that the co-expression of caveolins 1 and 2 is uncoupled by cellular transformation by activated oncogenes, such as v-Abl and activated H-Ras (G12V). While caveolin-1 mRNA and protein levels are down-regulated in response to cellular transformation (23), caveolin-2 protein levels remain relatively unchanged. While these cells continue to express caveolin-2 protein (this report), they fail to contain detectable caveolae, as we have reported previously (23). These observations suggest that caveolin-2 expression alone is not sufficient to drive the formation of morphologically detectable caveolae. However, detergent-insoluble caveolin-2-rich domains still exist (in the absence of caveolin-1) that are not distinguishable as "invaginated caveolae" by conventional transmission electron microscopy. These observations suggest that caveolin-rich microdomains may be more versatile structures with greater plasticity than previously imagined. In support of this idea, we have recently expressed caveolin-2 in Sf21 insect cells using baculo-virus-based vectors. Caveolin-2 expression in these insects cells fails to drive the formation of caveolae-like vesicles[2] while recombinant expression of caveolin-1 within the same cell system is sufficient to drive the formation of hundreds of uniform caveolae-like vesicles (50–100 nm in diameter) (18). These results are consistent with the idea that caveolin-2 may function as an "accessory protein" in conjunction with caveolin-1.

In many experiments we observed a slightly less abundant and faster migrating form of caveolin-2 (See Figs. 2, 3, and 4). This may represent a proteolytic degradation product of caveolin-2 or may be a translationally produced isoform. As a single caveolin-1 mRNA gives rise to caveolin-1α and caveolin-1β via alternate translation initiation (28), we favor the possibility that the faster migrating form of caveolin-2 is also generated as a consequence of alternate translation initiation. In support of this hypothesis, further sequencing and analysis of the 5′ end of the human caveolin-2 cDNA reveals an additional initiator methionine 13 amino acids upstream (MGLETEKADVQLFMDD.....) of the previously reported initiator methionine. The updated cDNA sequence can be found under GenBank™ accession number U32114. We are currently investigating the significance of this upstream initiation site. However, one possibility is that this upstream initiator may allow for myristoylation of caveolin-2 as an N-terminal cytoplasmic MG sequence is a co-translational consensus site for N-myristoylation. In addition, these two methionines may serve as alternate translation initiation sites to generate two distinct isoforms of caveolin-2 (Cav-2α and Cav-2β). If this is the case, then only the longer isoform of caveolin-2 (Cav-2α) would be expected to undergo myristoylation.

Caveolin-3 is a muscle-specific caveolin-related protein that is expressed in striated muscle cell types (cardiac and skeletal) (29–31). Unlike caveolin-3, caveolin-1 is not expressed in striated muscle cells. It was, therefore, surprising to observe caveolin-2 expression in three skeletal myoblast cell lines (L6, BC3H1, and C2C12) and in differentiated C2C12 myotubes. As caveolins-1 and -3 are most closely related based on primary sequence homology and caveolin-2 is most distant (30), caveolin-2 may also function in embryonic muscle as a complex with caveolin-3. However, we have been unable to demonstrate a

[2] M. P. Lisanti, unpublished observations.

stable association between caveolins 2 and 3 by co-immunoprecipitation (data not shown), as caveolin-2 is not expressed within adult skeletal muscle fibers (See Fig. 11).

Caveolins 1 and 3 may have originated from a common ancestor as we have recently identified only two caveolins within *C. elegans*, termed Cav^{ce}-1 and Cav^{ce}-2 (43). Cav^{ce}-1 is most closely related to mammalian caveolins-1 and -3; Cav^{ce}-2 is most closely related to mammalian caveolin-2 (43). Thus, caveolin-2 appears to be structurally and functionally conserved from worms to man, suggesting an important evolutionary role for caveolin-2 in the regulation of caveolae membranes.

Acknowledgments—We thank members of the Scherer and Lisanti laboratories for helpful and insightful discussions, Dr. Perry Bickel for donating anti-GDI antibodies, Michael Cammer for help with laser scanning confocal microscopy, Gina Georgescue for expert processing of human muscle biopsies, the darkroom services of Utrecht for printing of electron micrographs, and Drs. John R. Glenney, Jr., and Roberto Campos-Gonzalez for mAb production at Transduction Laboratories (Lexington, KY).

REFERENCES

1. Lisanti, M. P., Scherer, P., Tang, Z.-L., and Sargiacomo, M. (1994) *Trends Cell Biol.* **4,** 231–235
2. Couet, J., Li, S., Okamoto, T., Scherer, P. S., and Lisanti, M. P. (1997) *Trends Cardiovasc. Med.* **7,** 103–110
3. Fan, J. Y., Carpentier, J.-L., van Obberghen, E., Grunfeld, C., Gorden, P., and Orci, L. (1983) *J. Cell Sci.* **61,** 219–230
4. Scherer, P. E., Lisanti, M. P., Baldini, G., Sargiacomo, M., Corley-Mastick, C., and Lodish, H. F. (1994) *J. Cell Biol.* **127,** 1233–1243
5. Scherer, P. E., Okamoto, T., Chun, M., Nishimoto, I., Lodish, H. F., and Lisanti, M. P. (1996) *Proc. Natl. Acad. Sci. U. S. A.* **93,** 131–135
6. Simionescu, N., and Simionsecu, M. (1983) in *Histology: Cell and Tissue Biology* (Weiss, L., ed), Fifth Ed., pp. 371–433, Elsevier Biomedical, New York
7. Forbes, M. S., Rennels, M., and Nelson, E. (1979) *J. Ultrastruc. Res.* **67,** 325–339
8. Bretscher, M., and Whytock, S. (1977) *J. Ultrastruc. Res.* **61,** 215–217
9. Glenney, J. R., Jr. (1989) *J. Biol. Chem.* **264,** 20163–20166
10. Glenney, J. R., and Soppet, D. (1992) *Proc. Natl. Acad. Sci. U. S. A.* **89,** 10517–10521
11. Glenney, J. R. (1992) *FEBS Lett.* **314,** 45–48
12. Rothberg, K. G., Heuser, J. E., Donzell, W. C., Ying, Y., Glenney, J. R., and Anderson, R. G. W. (1992) *Cell* **68,** 673–682
13. Kurzchalia, T., Dupree, P., Parton, R. G., Kellner, R., Virta, H., Lehnert, M., and Simons, K. (1992) *J. Cell Biol.* **118,** 1003–1014
14. Sargiacomo, M., Scherer, P. E., Tang, Z.-L., Kubler, E., Song, K. S., Sanders, M. C., and Lisanti, M. P. (1995) *Proc. Natl. Acad. Sci. U. S. A.* **92,** 9407–9411
15. Monier, S., Parton, R. G., Vogel, F., Behlke, J., Henske, A., and Kurzchalia, T. (1995) *Mol. Biol. Cell* **6,** 911–927
16. Song, K. S., Tang, Z.-L., Li, S., and Lisanti, M. P. (1997) *J. Biol. Chem.* **272,** 4398–4403
17. Fra, A. M., Williamson, E., Simons, K., and Parton, R. G. (1995) *Proc. Natl. Acad. Sci. U. S. A.* **92,** 8655–8659
18. Li, S., Song, K. S., Koh, S., and Lisanti, M. P. (1996) *J. Biol. Chem.*, **271,** 28647–28654
19. Engelman, J. A., Wykoff, C. C., Yasuhara, S., Song, K. S., Okamoto, T., and Lisanti, M. P. (1997) *J. Biol. Chem.* **272,** 16374–16381
20. Murata, M., Peranen, J., Schreiner, R., Weiland, F., Kurzchalia, T., and Simons, K. (1995) *Proc. Natl. Acad. Sci. U. S. A.* **92,** 10339–10343
21. Li, S., Song, K. S., and Lisanti, M. P. (1996) *J. Biol. Chem.* **271,** 568–573
22. Fra, A. M., Masserini, M., Palestini, P., Sonnino, S., and Simons, K. (1995) *FEBS Lett* **375,** 11–14
23. Koleske, A. J., Baltimore, D., and Lisanti, M. P. (1995) *Proc. Natl. Acad. Sci. U. S. A.* **92,** 1381–1385
24. Li, S., Okamoto, T., Chun, M., Sargiacomo, M., Casanova, J. E., Hansen, S. H., Nishimoto, I., and Lisanti, M. P. (1995) *J. Biol. Chem.* **270,** 15693–15701
25. Li, S., Couet, J., and Lisanti, M. P. (1996) *J. Biol. Chem.* **271,** 29182–29190
26. Song, K. S., Li, S., Okamoto, T., Quilliam, L., Sargiacomo, M., and Lisanti, M. P. (1996) *J. Biol. Chem.* **271,** 9690–9697
27. Couet, J., Li., S., Okamoto, T., Ikezu, T., and Lisanti, M. P. (1997) *J. Biol. Chem.* **272,** 6525–6533
28. Scherer, P. E., Tang, Z.-L., Chun, M. C., Sargiacomo, M., Lodish, H. F., and Lisanti, M. P. (1995) *J. Biol. Chem.* **270,** 16395–16401
29. Song, K. S., Scherer, P. E., Tang, Z.-L., Okamoto, T., Li, S., Chafel, M., Chu, C., Kohtz, D. S., and Lisanti, M. P. (1996) *J. Biol. Chem.* **271,** 15160–15165
30. Tang, Z.-L., Scherer, P. E., Okamoto, T., Song, K., Chu, C., Kohtz, D. S., Nishimoto, I., Lodish, H. F., and Lisanti, M. P. (1996) *J. Biol. Chem.* **271,** 2255–2261
31. Way, M., and Parton, R. (1995) *FEBS Lett.* **376,** 108–112
32. Sargiacomo, M., Sudol, M., Tang, Z.-L., and Lisanti, M. P. (1993) *J. Cell Biol.* **122,** 789–807
33. Bickel, P. E., Scherer, P. E., Schnitzer, J., Oh, P., Lisanti, M. P., and Lodish, H. F. (1997) *J. Biol. Chem.* **272,** 13793–13802
34. Harlow, E., and Lane, D. (eds) (1988) *Antibodies: A Laboratory Manual*, Cold Spring Harbor Laboratory, Cold Spring Harbor, NY
35. Baldini, G., Hohl, T., Lin, H., and Lodish, H. F. (1992) *Proc. Natl. Acad. Sci. U. S. A.* **89,** 5049–5052
36. Cole, F., Fasy, T. M., Rao, S., Peralta, M., and Kohtz, D. S. (1993) *J. Biol. Chem.* **268,** 1580–1585
37. Blau, H., Chiu, C.-P., and Webster, C. (1983) *Cell* **32,** 1171–1180
38. Lisanti, M. P., Tang, Z.-L., and Sargiacomo, M. (1993) *J. Cell Biol.* **123,** 595–604
39. Peters, P. J., Neefjes, J. J., Oorschot, V., Ploegh, H. L., and Geuze, H. J. (1991) *Nature* **349,** 669–678
40. Liou, W., Geuze, H. J., and Slot, J. W. (1996) *Histochem. Cell Biol.* **106,** 41–58
41. Glenney, J. R., and Zokas, L. (1989) *J. Cell Biol.* **108,** 2401–2408
42. Scherer, P., Williams, S., Fogliano, M., Baldini, G., and Lodish, H. F. (1995) *J. Biol. Chem.* **270,** 26746–26749
43. Tang, Z., Okamoto, T., Boontrakulpoontawee, P., Katada, T., Otsuka, A., and Lisanti, M. (1997) *J. Biol. Chem.* **272,** 2437–2445

This Page is Inserted by IFW Indexing and Scanning Operations and is not part of the Official Record

BEST AVAILABLE IMAGES

Defective images within this document are accurate representations of the original documents submitted by the applicant.

Defects in the images include but are not limited to the items checked:

- ☐ BLACK BORDERS
- ☑ IMAGE CUT OFF AT TOP, BOTTOM OR SIDES
- ☑ FADED TEXT OR DRAWING
- ☐ BLURRED OR ILLEGIBLE TEXT OR DRAWING
- ☐ SKEWED/SLANTED IMAGES
- ☑ COLOR OR BLACK AND WHITE PHOTOGRAPHS
- ☐ GRAY SCALE DOCUMENTS
- ☑ LINES OR MARKS ON ORIGINAL DOCUMENT
- ☐ REFERENCE(S) OR EXHIBIT(S) SUBMITTED ARE POOR QUALITY
- ☐ OTHER: _____

IMAGES ARE BEST AVAILABLE COPY.
As rescanning these documents will not correct the image problems checked, please do not report these problems to the IFW Image Problem Mailbox.